Earth and Space Science

RESEARCH ARTICLE
10.1029/2019EA000873

Comparison of Six Lightning Parameterizations in CAM5 and the Impact on Global Atmospheric Chemistry

F. J. Gordillo-Vázquez[1], F. J. Pérez-Invernón[1], H. Huntrieser[2], and A. K. Smith[3]

[1]Instituto de Astrofísica de Andalucía (IAA), CSIC, Granada, Spain, [2]Institut für Physik der Atmosphäre, Deutsches Zentrum für Luft- und Raumfahrt, Wessling, Germany, [3]Atmospheric Chemistry Observations and Modeling, National Center for Atmospheric Research, Boulder, CO, USA

Key Points:
- Lightning schemes based on upward ice flux (ICEFLUX) and cloud top height (CTH) exhibit the largest spatial correlations with observation
- Five out of six lightning schemes tested with CAM5 exhibit larger LNO_x in midlatitudes than in tropics
- ICEFLUX can be considered a reliable lightning scheme when tested in CAM5

Supporting Information:
- Supporting Information S1

Correspondence to:
F. J. Gordillo-Vázquez,
vazquez@iaa.es

Citation:
Gordillo-Vazquez, F. J., Pérez-Invernón, F. J., Huntrieser, H., & Smith, A. K. (2019). Comparison of six lightning parameterizations in CAM5 and the impact on global atmospheric chemistry. *Earth and Space Science. 6*, 2317–2346. https://doi.org/10.1029/2019EA000873

Received 3 SEP 2019
Accepted 21 OCT 2019
Accepted article online 9 NOV 2019
Published online 9 DEC 2019

Abstract We present simulations performed with six lightning parameterizations implemented in the Community Atmosphere Model (CAM5). The amount of lightning-produced nitrogen oxides (LNO_x) by the various schemes considered is estimated. We provide some insight on how the lightning NO injected in the atmosphere influences the global concentrations of key chemical species such as OH, HO_2, H_2O_2, NO_x, O_3, SO_2, CO, and HNO_3. The vertical global averaged densities of HO_2, H_2O_2, CO, and SO_2 are depleted due to lightning while those of NO, NO_2, O_3, OH, and HNO_3 increase. Our results indicate that the parameterizations based on the upward ice flux (ICEFLUX) exhibit the largest global and midlatitude spatial correlations (0.73 and 0.632 for ICEFLUX and 0.72 and 0.553 for cloud top height) with respect to satellite global flash rate observations. Five out of the six lightning schemes investigated exhibit larger LNO_x per flash in the midlatitudes than in the tropics. In particular, it is found that the ICEFLUX midlatitude LNO_x per flash exhibits the largest difference with respect to its predicted tropical LNO_x per flash, in agreement with available observations. When using CAM5, the ICEFLUX lightning parameterization could be considered a reliable lightning scheme (within its intrinsic uncertainties) in terms of its geographical distribution. Both ICEFLUX and cloud top height results agree with the enhancements of NO_2 and O_3 produced by lightning over tropical Atlantic and Africa and the weaker lightning background over the tropical Pacific reported by Martin et al. (2007) in the periods and locations (upper troposphere) where lightning is expected to dominate the trace gas observations.

1. Introduction

Lightning is one of the most energetic natural phenomena taking place in the atmosphere of the Earth and one of the major sources of nitrogen oxides (NO_x = NO + NO_2) in the troposphere influencing the global atmospheric chemistry (Schumann & Huntrieser, 2007). In spite of this, the source rate of lightning-induced nitrogen oxides (LNO_x) remains not well known due to the difficulties in measuring it. Lightning contributes not only to the global amount of NO_x (Grewe et al., 2004; Liaskos et al., 2015) but also to the chemical balance of other important trace gases such as ozone (O_3) (Finney et al., 2016; Grewe, 2007; Wild, 2007), hydroperoxyl radical (HO_2), hydrogen peroxide (H_2O_2) or the hydroxyl radical (OH) (Labrador et al., 2004; Liaskos et al., 2015) that controls the oxidizing capacity of the atmosphere and the lifetime of many anthropogenic and natural molecular compounds (Schumann & Huntrieser, 2007). The influence of LNO_x on the global levels of other atmospheric chemical components such as, for instance, carbon monoxide (CO), nitric acid (HNO_3), or sulfur dioxide (SO_2), is not well known either.

Many studies in the last three decades have contributed to determine the amount of LNO_x by extrapolating local measurements of NO_x from single lightning or regional storms to the global scale (Apel et al., 2015; Chameides et al., 1987; DeCaria et al., 2005; Huntrieser et al., 1998; Price et al., 1997; Ridley et al., 2005) with the best estimate value to date of about 5 ± 3 Tg N $year^{-1}$ (given in nitrogen atom mass units per year) and an average value of 250 mol NO per flash (Schumann & Huntrieser, 2007).

Important efforts have been done during the last two decades (since late 1990s) in order to try to reduce the large uncertainty of the global LNO_x values and to understand the fundamental influence of upper tropospheric (UT) thunderstorm outflows on the UT and lower stratosphere (LS) O_3 and NO_x contents (Huntrieser et al., 2016a, 2016b). This progress has been possible due to the availability of lightning detection from space (Cecil et al., 2014; Christian et al., 2003) and satellite observations of global distribution

of NO_2 columns by instruments such as GOME Burrows et al. (1999), SCIAMACHY (Beirle et al., 2010; Bovensmann et al., 1999), OMI (Levelt et al., 2006; Pickering et al., 2016) or GOME-2, (Miyazaki et al., 2017). Also important are the numerous airborne multi-instrument measurements of thunderstorms mainly carried out since the mid-1980s in regions of North America (PRE-STORM in 1985, Luke et al., 1992, TRACE-A in 1992, Pickering et al., 1996, DC3 in 2012, Barth et al., 2015; Huntrieser et al., 2016a, 2016b; Pollack et al., 2016), South America (GTE/ABLE in 1985, (Torres & Buchan, 1988), (Baehr et al., 2003), TROCCINOX in 2004–2005, (Huntrieser et al., 2007), RELAMPAGO-CACTI in 2018–2019, (Nesbitt et al., 2017), and Africa (AMMA campaign in 2006 Redelsperger et al., 2006), where lightning activity is specially strong.

The availability since the 1990s of lightning observations from space (low-Earth orbit) has allowed to establish empirical relationships (parameterizations) between lightning frequency and meteorological variables. Some of these lightning schemes are based on the cloud top height (CTH) by Price and Rind (1992), maritime upgraded CTH or CTH-M (that improves the CTH geographical lightning flash distribution over the oceans) by Michalon et al. (1999), updraft strength (US) by Grewe et al. (2001), convective precipitation (CP) at the surface (for precipitation stronger than 7 mm/day) and on the upward mass flux (MFLUX) at 440 hPa both proposed by Allen and Pickering (2002). Other lightning parameterizations are based on a combination of convective precipitation and convective available potential energy (CPCAPE) by Romps et al. (2014), or on the upward ice flux at 440 hPa (ICEFLUX) by Finney et al. (2014). Scale factors are generally used to match the global lightning frequency (in flashes per minute) from different lightning parameterizations to the global lightning frequency reported by the Optical Transient Detector (OTD) and by the Lightning Imaging Sensor (LIS).

Since the mid-1990s global models and reanalysis data have been testing different lightning schemes. The study by Tost et al. (2007) using four lightning parameteriations (CTH, CP, MFLUX, and US)—with several convective schemes—in the ECHAM5/MESSy model showed a wide range in the spatial and temporal variability of the simulated lightning flash densities. This was attributed to both types (convective and lightning) of parameterizations.

The work by Finney et al. (2014) using five lightning parameterizations (including CTH, CP, MFLUX, and the new ICEFLUX scheme) with the same convective scheme throughout the ERA-Interim global atmospheric reanalysis data product (from 1989 to present) showed that ICEFLUX exhibited the greatest spatial correlations with observations. This resulted in a more realistic and better balance between the tropical and subtropical lightning flash densities.

A recent study by Clark et al. (2017) implemented eight lightning parameterizations in the Community Atmosphere Model version 5 (CAM5) to investigate their performance in present and future climate scenarios between 38°S latitude and 38°N latitude and with a 13-year analysis period. Clark et al. (2017) restricted their study to the analysis of the lightning frequency.

In the present paper we have explored not only the global lightning frequency but also how lightning affect the global atmospheric chemistry depending on the selected lightning parameterization. We have analyzed four of the lightning parameterizations (CTH, CTH-M, CP, and MFLUX) considered by Clark et al. (2017) plus the CPCAPE and ICEFLUX lightning schemes recently proposed by Romps et al. (2014, 2018) and Finney et al. (2014), respectively.

We use CAM5 to explore the influence of lightning on the global atmospheric chemistry. For this particular model, the different annual mean flash density productions by the six lightning parameterizations mentioned above have been calculated and validated. The validation is done by comparing the spatial correlation between 60°S latitude and 60°N latitude of the lightning flash rate predicted by each parameterization with available observations by OTD since 1995 and by LIS since 1997 until 2014 (Cecil et al., 2014; Christian et al., 2003). Once this is done, we compare our calculations of the considered lightning parameterization's LNO_x with the consensus estimate of 5 ± 3 Tg N $year^{-1}$ (Schumann & Huntrieser, 2007). Since 2007, a number of LNO_x estimates based on satellite observations have also become available (Beirle et al., 2006, 2010; Martin et al., 2007) and more recently the work by Marais et al. (2018) with a satellite-based estimate for LNO_x of 5.9 ± 1.7 Tg N $year^{-1}$ located at the lower edge of the range given by Schumann and Huntrieser (2007). Also some recent estimates have been published of ~9 Tg N $year^{-1}$ (Nault et al., 2017), that are located just above the upper edge of the range given by Schumann and Huntrieser (2007). Their higher estimate is connected to a shorter lifetime of NO_x than considered until recently.

Important trace gases for the lightning chemistry are NO, NO_2 that influence on the abundances of O_3, OH, HO_2, and H_2O_2. The hydroxyl radical (OH) is a key agent in the oxidizing capacity of the atmosphere which controls the global concentration of tropospheric O_3 and H_2O_2 and influences the lifetime of a large number of anthropogenic and natural compounds like CO and SO_2. Under clean air conditions, OH is mainly produced by O_3 photolysis and reactions of the resultant atomic oxygen with water vapor. Under more polluted conditions in the troposhere, OH is also formed by photolysis of NO_2 during the oxidation of CO and methane (CH_4) and nonmethane hydrocarbons (Schumann & Huntrieser, 2007). In "NO_x-saturated" regions, an increase of NO_x, by reactions with HO_2 and NO_2, reduces the HO_2/OH ratio, and the production rate of O_3 (Schumann & Huntrieser, 2007). Finally, part of the NO_2 reacts with OH producing HNO_3.

The next section describes CAM5, the various lightning parameterizations considered, the simulation procedure followed and the type of lightning data used. Section 3 is devoted to evaluate and discuss the results obtained by comparing the different lightning schemes and the impact of lightning on the global concentrations of chemical species. This is followed by a summary and conclusions section.

2. Model and Lightning Data

We use the Community Atmosphere Model version 5 (CAM5) that covers the altitude range from the surface up to approximately 3.6 mbar (≃40 km). This is of interest because, though lightning sources stay in the troposphere, transport mechanisms could move lightning chemistry products to higher altitudes (LS). For this reason our simulations extend up to ≃40 km (though we only show altitude plots up to 30 km).

CAM5 is the atmospheric component of the Community Earth Climate System Model (CESM Version 1.2) and includes all the physical parameterizations of CAM4 (Marsh et al., 2013; Tilmes et al., 2015) plus many other physical processes and improvements not included in CAM4 like tropical convection (Tilmes et al., 2015).

CAM5 is fully coupled to tropospheric and stratospheric chemistry, referred hereafter as CAM5-Chem, and shows a reasonable representation of present-day atmospheric composition in the troposphere and stratosphere (Tilmes et al., 2015). The atmospheric chemistry in CAM5-Chem is based on Version 4 of the Model for OZone And Related chemical Tracers (MOZART 4) for the troposphere (Emmons et al., 2010) including extended stratospheric chemistry (Kinnison et al., 2007) and further updates (Lamarque et al., 2012; Tilmes et al., 2015) together with the Modal Aerosol Model with three modes (MAM3) (Liu et al., 2012). CAM5-Chem considers 183 species (plus 25 more introduced by MAM3) and 472 chemical reactions including photolysis, gas-phase (neutral and ionic) chemistry and heterogenous chemistry in both the troposphere and LS. The reaction rates used are those of the JPL2010 recommendations (Sander et al., 2011).

2.1. Lightning Parameterizations

General Circulation Models (GCMs) do not explicitly simulate the microphysics of the electrification process in thunderstorms producing lightning nor their subsequent production of NO_x and its coupling to the tropospheric and stratospheric chemistry. Therefore, since lightning is treated as subgrid atmospheric phenomenon in GCMs, lightning frequencies (number of flashes per minute within a grid box at a given latitude and longitude) and also, sometimes, the associated NO_x production are parameterized as a function of different meteorological variables in the models. At present there are no global models which explicitly simulate the storm electrification process. The use of lightning schemes introduces uncertainties (that one need to be aware of) in the modeling of lightning frequency together with the lightning NO_x formation and resultant tropospheric chemistry.

Moreover, global models do not simulate either the microphysics and chemical output of new types of transient atmospheric electrical phenomena such as Sprites (Franz et al., 1990), Blue Jets (Gordillo-Vázquez & Donkó, 2009; Wescott et al., 1995), Halos (Parra-Rojas et al., 2013) and Elves (Inan et al., 1997; Pérez-Invernón et al., 2018). The global chemical impact of Sprites (Arnone et al., 2014) and Blue Jets (Pérez-Invernón et al., 2019) has been recently explored with GCMs.

By default CAM5 uses the CTH lightning parameterization (Price & Rind, 1992). We have evaluated a total of six lightning parameterizations in CAM5 using scale factors to match the global lightning frequency (in flashes per minute) resulting from each of the lightning parameterizations considered to the global lightning frequency observed by OTD/LIS. Two of the lightning parameterizations are based on the convective CTH above ground, hereafter called the CTH lightning scheme proposed by Price and Rind (1992) following

previous investigations by Vonnegut (1963) and Williams (1985) showing that lightning frequencies in continental thunderstorms are related to the fifth power of the cloud height. Because of the difference in cloud dynamics between the continental and oceanic thunderstorms (maximum updrafts of continental and martitime storms are, respectively, 50–60 m/s and 10 m/s) Price and Rind (1992) also proposed a new lightning parameterization for marine thunderclouds after establishing a connection between the very weak updraft velocity in marine thunderstorms (Jorgensen & LeMone, 1989) and marine convective cloud heights. However, due to the scarce observations of marine thunderstorms available in 1992, the maritime CTH lightning parameterization considerably underestimates global observations reported later from space by OTD/LIS. In this regard, the lightning parameterization proposed by Michalon et al. (1999), hereafter called CTH-M, is a variation of the CTH lightning parameterization accounting for a correction of the CTH maritime lightning flash frequency.

Two additional lightning schemes used in this work are based on the CP at the surface (only for precipitation amounts stronger than 7 mm/day), hereafter called CP, and on updraft mass flux at 440 hPa, hereafter called MFLUX (Allen & Pickering, 2002).

Finally, we have also considered two recently proposed lightning parameterizations. One by Romps et al. (2014, 2018), hereafter called CPCAPE, based on the product of the CP and the convective available potential energy (CAPE), and another one by Finney et al. (2014), hereafter called ICEFLUX, based on the upward ice flux-lightning relationship. The ICEFLUX scheme motivated by previous results by Deierling et al. (2008) showing that the upward ice flux displays a strong linear correlation with lightning flashes in a number of observed storms in the US. The lightning parameterization by Finney et al. (2014) used here provides two linear fits correlating the total lightning flash density of land ($f_l = 6.58 \times 10^{-7}\phi_{ice}$) and ocean ($f_o = 9.08 \times 10^{-8}\phi_{ice}$) with the upward cloud ice flux (ϕ_{ice}) at 440 hPa.

Of the six tested lightning schemes, only three (CTH, CTH-M and ICEFLUX) have separate parameterizations for land and ocean.

Five of the eight lightning schemes considered in the recent study by Clark et al. (2017) using CAM5 were variations of the CTH parameterization by Price and Rind (1992), the other three were a cold cloud depth (CCD)-based scheme by Yoshida et al. (2009), and the CP and MFLUX schemes proposed by Allen and Pickering (2002). The results by Clark et al. (2017) indicate that in the present day, the annual mean lightning flash densities in simulations constrained by reanalysis data show the highest global spatial correlation (r) to satellite observations for lightning schemes based either on CTH ($r = 0.83$) or CCD ($r = 0.80$). Under future scenarios, changes in global mean flash density are highly sensitive to the lightning scheme chosen, with CTH schemes, a CCD scheme, and a scheme based on convective mass flux projecting large increases, a mild increase and a decrease in lightning flash density, respectively (Clark et al., 2017; Finney et al., 2018).

2.2. Lightning NO_x Calculation

Price and Rind (1993) showed that the ratio between intracloud (IC) and cloud-to-ground (CG) lightning is linked to the thickness of the cold cloud region in thunderclouds (between 0 °C and cloud top), rather than to the freezing level height. Price et al. (1997) presented the first global and seasonal distribution of lightning-produced NO_x (LNO_x) based on the physical features of lightning strokes and on calculated global lightning frequencies derived from the observed distribution of electrical storms provided by the International Satellite Cloud Climatology Project (Rossow & Schiffer, 1991) between 1983 and 1991.

We have assumed a mean energy per CG and IC flash of, respectively, 6.7×10^9 J and 6.7×10^8 J, and a NO molecule production rate per discharge energy of 10^{17} molecules NO/J, (Price et al., 1997), that is, we consider here that CG lightning produces 10 times more NO than ICs, with 6.7×10^{26} molecules of NO per CG flash and 6.7×10^{25} molecules of NO per IC flash. The assumption that there is a significant difference between the IC and CG flash productions of NO is supported by theoretical and model estimates (Carey et al., 2016; Koshak et al., 2014; Pickering et al., 1998; Price et al., 1997). The recent paper by Koshak et al. (2014) presented results from the National Aeronautics and Space Administration Lightning Nitrogen Oxides Production model—using theoretical and laboratory findings along with lightning mapping array (LMA) data—that supports substantial differences between the IC and CG lightning production of NO (Pickering et al., 2016). This analysis is further extended in Koshak (2014) using 9 years of North Alabama LMA and National Lightning Detection Network data and obtained mean CG production of 604 mol per flash and mean IC production of 38 mol per flash (Pickering et al., 2016). These important differences are

moderated by previous cloud/chemistry modeling-based studies constrained by regional anvil aircraft observations that found smaller differences between the source strengths of IC and CG flashes (DeCaria et al., 2005; Ott et al., 2007, 2010) that were extrapolated to estimations considered valid globally. Finally, very high frequency LMAs show longer average channel lengths for CGs than ICs, and longer channel length also means more LNO_x (Koshak et al., 2014). CGs also have larger currents than ICs, which is related with more LNO_x production.

Acoustic data indicate that IC discharges are less energetic than CG ones (Holmes et al., 1971; Rakov & Uman, 2003). One reason could be the decrease of the threshold value for electrical breakdown with altitude (Schumann & Huntrieser, 2007). Moreover, the NO production seems to decrease with decreasing ambient pressure for the same energy and peak current (Goldenbaum & Dickerson, 1993; Wang et al., 1998). Therefore, the productivity ratio IC LNO_x/CG LNO_x has been assumed to be 0.1 in early studies based on estimates of cloud charges, electrostatic potentials and acoustical measurements of the energy of CG and IC discharges (Kowalczyk & Bauer, 1981; Price et al., 1997), and this value has been used in many follow-on studies (see Table 12 in Schumann & Huntrieser, 2007). On the other hand, some relatively recent analyses of lightning observations and airborne measurements during STERAO (DeCaria et al., 2000), EULINOX (Fehr et al., 2004; Ott et al., 2007), and CRYSTAL-FACE (Ott et al., 2005) with cloud model simulations indicate that IC flashes produce about the same amount of NO as CG flashes (see Table 19 in Schumann & Huntrieser, 2007). Note that the higher (close to 1) IC LNO_x to CG LNO_x ratio for STERAO and EULINOX were derived using the ONERA very high frequency lightning detection system (Defer et al., 2001), which may overestimate the z = IC/CG ratio. The derived IC LNO_x/CG LNO_x ratio could be even higher when the z = IC/CG ratio is smaller (Schumann & Huntrieser, 2007). In contrast, the recent paper by Koshak et al. (2014) shows results from the National Aeronautics and Space Administration Lightning Nitrogen Oxides Production model—using theoretical and laboratory findings along with LMA data—that supports substantial differences between the IC and CG lightning production of NO (Pickering et al., 2016), being this the option chosen in this work. This election keeps consistency with the vertical distribution of lightning NO_x used in the preset work and originally proposed by Pickering et al. (1998) (that also adopted the assumption of IC flashes being 10% as energetic as CG flashes).

Being the above said, one needs to be aware that the IC LNO_x/CG LNO_x ratio remains uncertain in the scientific literature and that the election—also adopted by Pickering et al. (1998)—of IC flashes being 10% as energetic as CG flashes have an influence in the vertical distribution of lightning NO_x (Pickering et al., 1998) as well as in the lightning-produced chemical calculations. As stated by Pickering et al. (1998), if IC flashes contained less than 10% energy as CG flashes, the UT peak in the mass profiles might not be as pronounced.

The procedure followed to predict the LNO_x per flash is based on (1) the computation with CAM5 of the cold cloud thickness (region where the temperature goes from 0 °C to cloud top) followed by (2) the calculation of the z = IC/CG ratio using the empirical relationship (Price & Rind, 1993):

$$z = \frac{IC}{CG} = AdH^4 + BdH^3 + CdH^2 + DdH + E \quad (1)$$

where dH stands for the cold cloud thickness, $A = 0.021$, $B = -0.648$, $C = 7.493$, D =-36.54, and $E = 63.09$. The proportion (%) of total lightning which is CG is given by $p = 1/(z+1)$ (Price & Rind, 1993). The polynomial fit of equation (1) is only valid within the range of observed values, that is, 5.5 km < dH < 14 km (Price & Rind, 1993). The relationship (1) shown above between the IC/CG ratio and the cold cloud thickness was established using data for 139 thunderstorms in the western United States (US) during the summer of 1988 with a correlation factor of $r = 0.81$ (Price & Rind, 1993). Note that because equation (1) was derived for the conditions of the western United States, its applicability to other regions of the world need to be taken with care. The IC/CG ratio in different regions of the world might exhibit significant differences with respect to equation (1) due to a number of factors like temperature, humidity, and geography. However, we have the opinion that—even with equation (1) being only strictly valid for the region of the world (part of North America) used for its derivation—it can be very illustrative for the readers to see approximate trends of the IC/CG ratio that can provide insights on how LNO_x is distributed between IC and CG lightning. A final remark on equation (1) is that it was used in Pickering et al. (1998) to derive their vertical distribution of lightning NO_x that we have also adopted in this work (see section on lightning frequency). Pickering et al. (1998) state that there are uncertainties in the application of equation (1) for periods of a few minutes throughout the evolution of a storm.

Since some tested schemes (CTH, CTH-M, and ICEFLUX) provide the total lightning flash frequency (CG + IC), while others (CP, CPCAPE, and MFLUX) only give the CG lightning flash frequency, we followed a number of steps (detailed below) to compute the IC/CG ratio: (1) Use CAM5 to compute the cold cloud thickness, from which we derive (using equation (1)) the z = IC/CG ratio, (2) if only CG is known (for CP, CPCAPE, and MFLUX) we get IC flash counts from the computed IC/CG ratio, (3) if CG + IC is known (CTH, CTH-M, and ICEFLUX), we get the proportion (p) of total lightning which is CG, that is, $p = 1/(1+z)$ = CG/(IC + CG). Once we have individual CG and IC flash counts for each lightning scheme, we (4) evaluate the global LNO_x production (using equation (15) in Price et al., 1997) for each lightning scheme and, finally, (5) divide the LNO_x global production by CG and IC flash counts to get LNO_x/CG and LNO_x/IC, respectively. Therefore, the IC/CG ratio is not prescribed in our study but calculated (using equation (1)) from the cold cloud thickness computed with CAM5.

Once we have calculated the LNO_x, we need to place it in the atmosphere according to a vertical distribution. For this, we used the vertical distribution of LNO_x emissions recommended by Pickering et al. (1998). Other troposphere LNO_x vertical distributions such as the one proposed by Ott et al. (2010) places too much NO_x in the middle troposphere and not enough in the upper troposphere as recently pointed out by Nault et al. (2017) and previous studies by Allen et al. (2012) and Seltzer et al. (2015).

Note that the lightning-produced nitrogen oxide and the resulting atmospheric chemistry will depend on the assumptions made for NO from IC and CG flashes and from the vertical profile employed. In this regard, as pointed out by Pickering et al. (1998), uncertainties in the lightning NO_x profiles stem from a variety of sources: the type of events studied, the model (Goddard Cumulus Ensemble or GCE) used by Pickering et al. (1998) and the parameterization of lightning and NO_x production. The convective events simulated by GCE in Pickering et al. (1998) are representative of well-organized, relatively long-lived mesoscale convective systems (MCSs) for which cloud-resolving models (including GCE) generally perform well. Other types of convective events (like air mass tunderstorms, supercells or mesoscale convective complexes) are not well-simulated with cloud models. However, Pickering et al. (1998) indicates that the types of convection not simulated with GCE would produce roughly similar types of profiles as the ones calculated in Pickering et al. (1998). Uncertainties also exist in the parameterization of lightning and NO_x production in the GCE model used by Pickering et al. (1998). As stated there, Price et al. (1997) indicate approximately factor of 2 uncertainty in both the energy per flash and the number of NO molecules produced per unit energy. Therefore, uncertainties of these magnitudes will be reflected in Pickering et al. (1998)—and in the present work lightning NO_x mixing ratio results—due to these production uncertainties. According to Pickering et al. (1998), if actual NO production is greater or smaller than the values assumed there (and also in the present work), presumably the mixing ratios would be scaled up or down accordingly, and the shapes of the vertical profiles of lightning NO_x mass distributions would remain the same. Finally, as also stated in Pickering et al. (1998), the assumption of IC flashes being 10% as energetic as CG flashes does have an influence on the resulting profiles. If, for example, IC flashes contained less than this amount of energy, the UT peak in the mass profiles might not be as pronounced (Pickering et al., 1998).

By default CAM5 uses the CTH lightning parameterization (Price & Rind, 1992) but the globally averaged LNO_x source is usually adjusted to some preselected value to ensure total annual LNO_x nitrogen mass emission rate of approximately 5 ± 3 Tg N year^{-1} considered as a plausible estimate for present-day atmospheric conditions (Schumann & Huntrieser, 2007; Tilmes et al., 2016). In our study we have used scale factors to match the global flash frequency of the different lightning parameterizations considered to that observed by OTD/LIS but without preselecting globally averaged LNO_x sources.

2.3. Model Simulations

CAM5 has an option for nudging the meteorological fields, known as Specified Dynamics, or SD CAM5 (Tilmes et al., 2015). In this study, we use the facility of SD but, instead of nudging to reanalysis fields, we nudge to the meteorological fields from a previous (free-running) CAM5 simulation. The reason for using SD is to ensure that the basic dynamics in the lower and middle atmosphere is identical in simulations in which other changes are made.

The nudging is applied up to 40 km. The simulation procedure is as follows. First, we run CAM5 in free-running dynamic mode without considering lightning. Then, we run a second CAM5 simulation also without lightning but now using the SD mode, that is, the horizontal wind and temperature fields in the troposphere and stratosphere are nudged at each model time step of the previous (first) free-running dynamic CAM5 run. Finally, we run a third SD CAM5 simulation (considering lightning) that is nudged to the first free-running dynamics CAM5 run. We repeat the third simulation previously mentioned for each of the six different lightning parameterizations considered and we always compare their results with those of the second SD CAM5 runs; that is, we carry out comparisons between simulations of the atmosphere with and without lightning. All the simulations represent a "present-day" year using climatological sea surface temperatures computed over monthly averages between the year 1982 and 2001. The convection scheme used here is that reported by Zhang and McFarlane (1995) with improvements in the convective momentum transport (Richter & Rasch, 2008), which improved surface winds, stresses and tropical convection (Tilmes et al., 2016). The convection parameterization was kept constant for the six lightning parameterizations considered. The model was implemented with 30 levels, a time step of 30 min and a horizontal resolution of 2.5° longitude and 1.9° latitude.

The globally averaged LNO_x sources obtained with the six lightning parameterizations in CAM5 are not adjusted to any preselected value. In addition, as mentioned above, the uncertainty in the vertical distribution of LNO_x can affect the chemical response of the atmosphere.

2.4. Lightning Data

To compare the lightning flash frequency predictions of the different lightning schemes implemented in CAM5, we have used a combination of OTD and LIS lightning observations from 4 May 1995 to 31 December 2014. In particular, we have used the LIS/OTD Gridded Lightning Climatology Data Collection, Version 2.3.2015, High Resolution Monthly Climatology, which provides mean flash rates in the middle of each month (with a mean global flash rate from the merged climatology of 46 lightning flashes s^{-1}) with monthly smoothing on a 0.5° horizontal resolution (Cecil et al., 2014).

It is also worth mentioning that although the OTD/LIS lightning climatology is a major step forward in global lightning observations, it is still a low-Earth orbit data set and some observation and coverage uncertainties remain. This means that many individual orbits are combined in an attempt to infer the true flash count in any particular region or grid cell. Although there are sufficient orbits to adequately sample the entire diurnal cycle of lightning for a particular region, but nonetheless, the OTD and LIS did not continuously monitor any region or grid cell nor is the flash detection efficiency 100% for regions directly observed, and therefore, the OTD/LIS climatology still only represents a very good approximation to the real global lightning flash distribution (whenever OTD or LIS look in one limited region, they are not technically seeing what is happening anywhere else on Earth).

Therefore, since the OTD/LIS climatology can present some (probably small) error bars, we should have some care in establishing the performance of the six lightning schemes, especially when some of them perform similarly (as we will see later).

For the first time, continuous monitoring from the Geostationary Lightning Mapper—and also from the European Geostationary Lightning Imager (LI) in the near future—can be used to evaluate the lightning climatology to be established by the International Space Station LIS, and this will help retroactively to shed light on the accuracy of the standard OTD/LIS climatology over the observed regions.

3. Results and Discussion

In this section we show the results obtained for the six different lightning parameterizations implemented in CAM5. We discuss the calculated annual average flash density for a "present-day" year (see section 2.3) for each of the lightning parameterizations considered and will compare them with available observations of annual mean flash rates (section 3.1). We also compare the influence of the different lightning parameterizations on the vertical (section 3.2) and horizontal (section 3.3) distribution (globally annually averaged) of the nine chemical species mentioned before in the introduction.

3.1. Global Distribution of Lightning Frequency and Lightning-Produced NO_x

3.1.1. Lightning Frequency

The scale factors mentioned above to match predicted and observed lightning flash densities for the different lightning schemes can show a wide range of variation. This depends on the global model used, its spatial

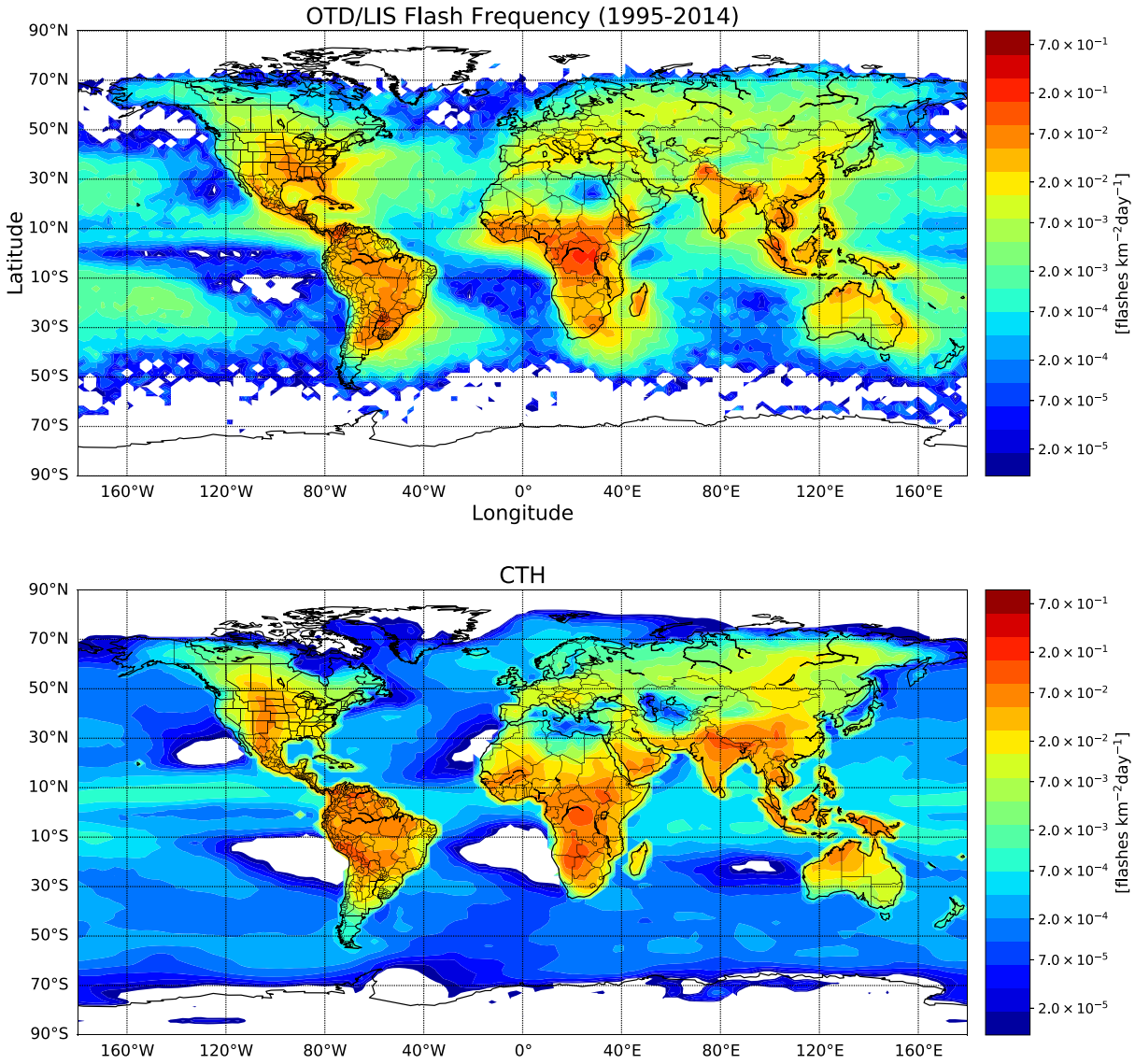

Figure 1. Global annual lightning observations by OTD/LIS using the LIS/OTD Gridded Lightning Climatology Data Collection, Version 2.3.2015, High Resolution Monthly Climatology (HRMC) from 4 May 1995 to 31 December 2014 degraded to that of the model resolution (2.5° longitude × 1.9° latitude) (upper panel) and calculated global annual average flash density for the convective cloud top height (CTH)-based lightning parameterization by Price and Rind (1992) (lower panel). Note that logarithmic scale is used, and consequently, zero values are not included. White regions correspond to numerical values that are below the minimum of the scale (10^{-5} flashes km^{-2} day^{-1}).

resolution, the particular convective scheme adopted or, as mentioned by Finney et al. (2014), on the different scales and regions where a particular lightning parameterization was developed. The study by Tost et al. (2007) using four lightning parameteriations (and five different convective schemes for each of them) in the ECHAM5/MESSy model with a 2.8° × 2.8° horizontal resolution shows that the scaling factors needed to match the global average number of flashes per second can vary in up to 3 orders of magnitude. The work by Finney et al. (2014) using five lightning parameterizations with the same convective scheme throughout the ERA-Interim reanalysis data product (from 1989 to present), interpolated with a regular 0.75° lat-lon grid, results in a global annual scaling factor (to match the global flash rate of 44 flashes s^{-1} of the LIS Low Resolution Full Climatology product) that varies by 2 orders of magnitude depending on the lightning parameterization. Finally, recent results by Finney et al. (2016), using the UK Chemistry and Aerosol (UKCA) model coupled to the atmosphere-only version of the UK Met Office Unified Model 8.4 run with a horizontal resolution of 1.875° lon × 1.25° lat, finds that the global flash rate scaling factors needed in the UKCA model are, respectively, 1.44 and 1.12 for the CTH and ICEFLUX lightning parameterizations. While

Table 1
Predicted Global Lightning-Produced NO_x in mol $flash^{-1}$ and Tg N $year^{-1}$ Together With the Global and Land/Ocean Spatial Correlations Between Observed and Predicted Flash Frequency Distributions

Lightning scheme	Predicted LNO_x (mol $flash^{-1}$)	Mean IC/CG	Predicted LNO_x (Tg N $year^{-1}$)	Consensus LNO_x (Tg N $year^{-1}$)	Spatial correlation land (r_l)/ocean (r_o)	Spatial correlation global (r)	Scale Factor
CTH[(1)]	328	3.80	6.5	5 ± 3	0.726/0.756	0.729	2.05
CTH-M[(2)]	322	3.94	7.0	5 ± 3	0.718/0.684	0.712	1.61
CP[(3)]	312	4.19	5.9	5 ± 3	0.493/0.367	0.448	1.72
MFLUX[(4)]	441	2.15	8.5	5 ± 3	0.412/0.431	0.415	1.80
CPCAPE[(5)]	302	4.24	6.0	5 ± 3	0.580/0.278	0.388	1.20
ICEFLUX[(6)]	337	3.60	6.8	5 ± 3	0.738/0.723	0.732	4.00

Note. The table shows the results of calculations done with CAM5 using each of the six lightning parameterizations. Note that the observed lightning frequency in the OTD/LIS time interval (May 1995 to December 2014) of the lightning climatology (HRMC) used for comparison is 46 flashes s^{-1}. The predicted mean ratio of intracloud to cloud-to-ground lightning flash frequencies is given by the column stating "Mean IC/CG" for each lightning scheme. The spatial correlation (r) is a parameter ranging from 0 to 1 accounting for similarity in the spatial distribution of the global (or land and ocean) flash density of each implemented lightning scheme in CAM5 with respect to the spatial distribution of the observed LIS/OTD lightning flash distribution. The mathematical equation for r is $\frac{\sum_i (x_i - \langle x \rangle)(y_i - \langle y \rangle)}{(\sum_i (x_i - \langle x \rangle)^2 \sum_i (y_i - \langle y \rangle)^2)^{0.5}}$, where x_i and y_i are the lightning frequencies in a cell domain i according to LIS/OTD and according to our simulations, respectively, and <x> and <y> stand for mean values per square kilometer. The predicted lightning flash rates range between 44 (CP) and 51 (CTH-M) flashes s^{-1}, and they were scaled to match the observations by OTD/LIS. The last column shows the scale factor used. The superscripts in the first column stand for the reference of the lightning scheme: (1) Price and Rind (1992), (2) Michalon et al. (1999), (3) and (4) Allen and Pickering (2002), (5) Romps et al. (2014), (6) Finney et al. (2014).

the scaling needed for the ICEFLUX parameterization in the UKCA model is similar (1.12) (Finney et al., 2016) to one earlier reported (1.09) when using ERA-Interim global atmospheric reanalysis data (Finney et al., 2014), there is a nonnegligible difference in the global flash rate scaling factors for the CTH parameterization when implemented in the UKCA, the ECHAM5/MESSy models and the present study (scale factor of 2.05). Global UKCA and ECHAM5/MESSy flash rate scaling factors of, respectively, 1.44 and a minimum of 0.74 (higher for different convection schemes) are more than one order of magnitude higher than that found (0.05) using the ERA-Interim data (Finney et al., 2014).

There are different procedures to calculate scaling factors. It is possible to find regional scaling factors, seasonal scaling factors, etc. Following previous studies, we have calculated a global annual scaling factor for each lightning scheme. The procedure followed to obtain the general scaling factors that we have used is (1) we run a 1-year simulation for each of the tested lightning schemes using the SD mode of CAM5. We nudge to the meteorological fields from a previous (free-running) CAM5 simulation without lightning. We obtain a global annually averaged occurrence rate of lightning discharges (f_{param}). (2) We calculate the scaling factor of the tested schemes as $f_{OTD-LIS}/f_{param}$, where $f_{OTD-LIS} = 46$ flashes s^{-1} is the global annually averaged occurrence rate of lightning discharges according to the chosen OTD/LIS lightning climatology. (3) We run the final simulations using the obtained scaling factors in Step 2. These scaling factors are applied (as multiplicative factors) to the equation that relates the lightning flash frequency with a/several meteorological variable/s according to each lightning parameterization.

Figure 1 (upper panel) shows the annual OTD and LIS lightning observations using the global annual mean flash rates in the middle of each month as provided by LIS/OTD Gridded Lightning Climatology Data Collection, Version 2.3.2015, High Resolution Monthly Climatology from 4 May 1995 to 31 December 2014. The latitudes covered go from 70°S to 70°N. The observed maxima take place over the continents, in central Africa, South America, central and east of North America, and some regions in the north of India and Southeast Asia.

Figure 1 (lower panel) shows the calculated global annual average flash density for the CTH parameterization based on the convective CTH which is the most widely used lightning scheme. Our 1-year simulation of the CTH parameterization with CAM5 produces 46 lightning flashes s^{-1} (scale factor of 2.05 with a high

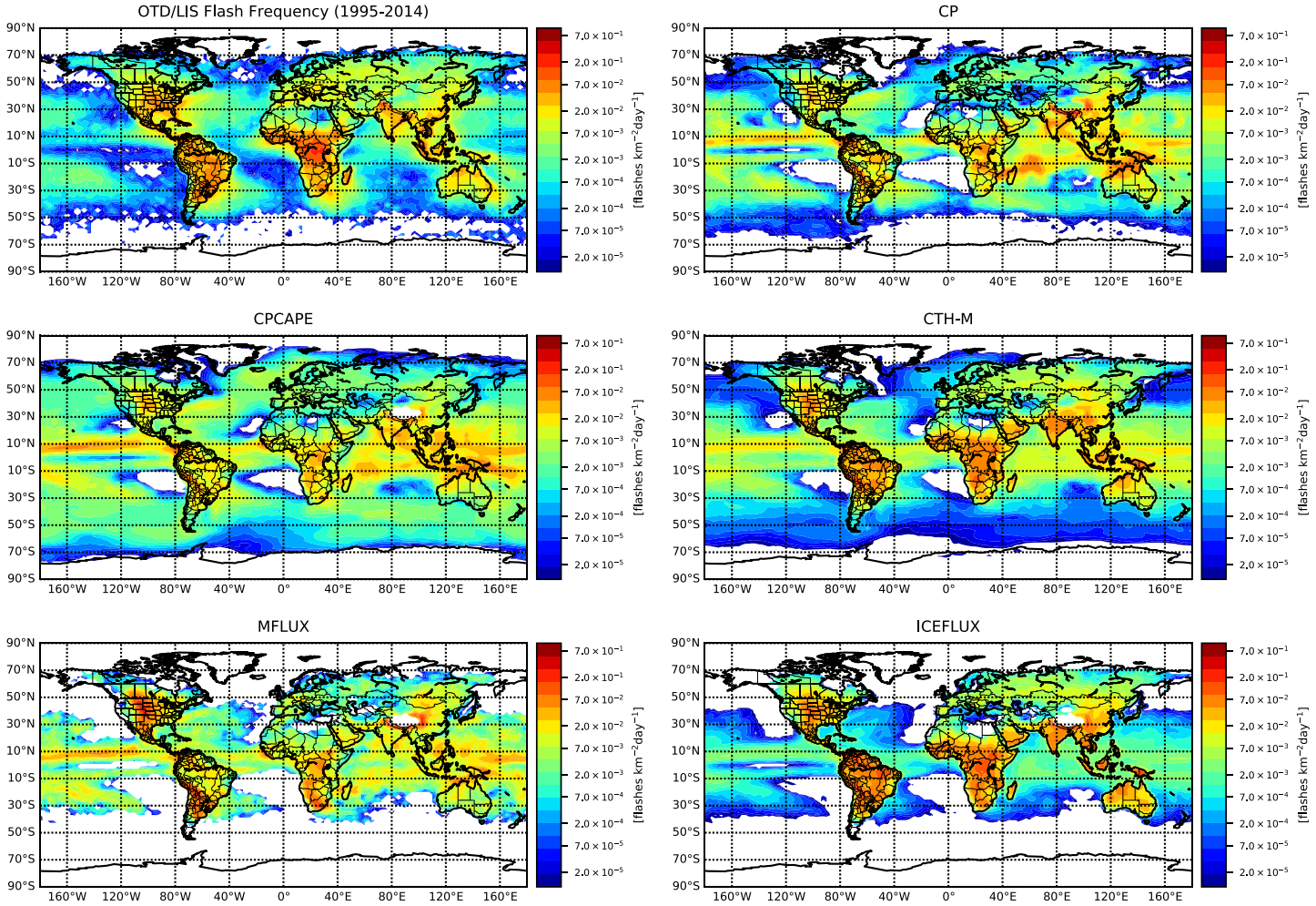

Figure 2. Comparison of the observed 1995–2014 LIS/OTD global annual average flash rates with five of the lightning parameterizations implemented in CAM5 correspoding to, respectively, the convective precipitation (CP)-based parameterization by Allen and Pickering (2002), the convective precipitation and CAPE (CPCAPE)-based parameterization by Romps et al. (2014), the parameterization by Michalon et al. (1999) consisting in the CTH parameterization by Price and Rind (1992) and an ocean flash rate upgrade (CTH-M) with respect to CTH, the updraft mass flux (MFLUX)-based parameterization by Allen and Pickering (2002), and the upward cloud ice flux (ICEFLUX)-based parameterization by Finney et al. (2014). Note that the spatial resolution (0.5° × 0.5°) of LIS/OTD observations has been degraded to that of the model resolution (2.5° longitude × 1.9° latitude). Note that logarithmic scale is used, and consequently, zero values are not included. White regions correspond to numerical values that are below the minimum of the scale (10^{-5} flashes km^{-2} day^{-1}).

global spatial correlation of 0.729, see Table 1) showing a clear contrast between ocean and land. The maritime flash densities are underestimated, while land flash densities are overestimated. However, the high land (0.726) and ocean (0.756) spatial correlations of the CTH lightning parameterization indicate that, though underestimated in ocean, the predicted CTH geographical distribution of lightning is quite close to the observations.

Figure 2 shows a comparison of the observed LIS/OTD global annual average flash rates with five of the lightning parameterizations implemented in CAM5. The precipitation-based lightning parameterization by Allen and Pickering (2002) (CP) produces 44 lightning flashes s^{-1} (scale factor of 1.72 with a global spatial correlation of 0.448) but underestimates the flash frequency over tropical central Africa and overestimates it over the tropical regions of South America and Southeast Asia including the Indian Ocean. On the other hand, in the midlatitudes continental lightning is underestimated except in Australia where the lightning distribution is reasonably better captured. This parameterization slightly overestimates lightning flash rate over the oceans. The CP parameterization land (0.493)/ocean (0.367) spatial correlations are quite different, being much higher over land than over the oceans.

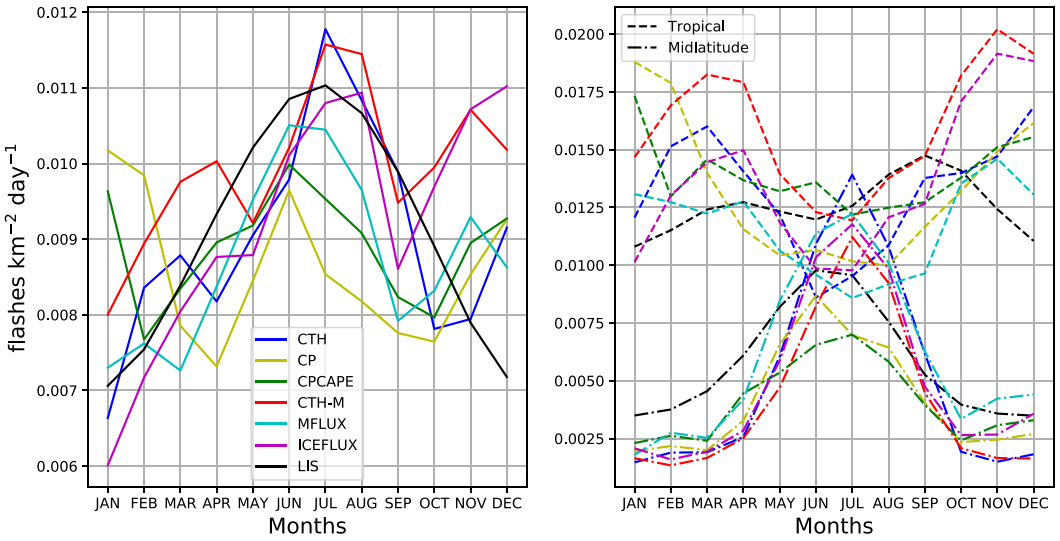

Figure 3. (Left panel) Monthly global average (60°S to 60°N) of the lightning flash density rate (flashes km^{-2} day^{-1}). The plot shows the comparison between the observed LIS lightning flash rate (dashed line) and the six different lightning schemes implemented in CAM5. The value shown in each month label corresponds to the mean between the first and the last day of the month (both for LIS and for the simulated results). (Right panel) Monthly tropical (25°N to 25°S, dashed line) and midlatitude (dashed dotted line) flash density rates for the six lightning schemes tested and the OTD/LIS climatology.

The CP times CAPE-based lightning parameterization by Romps et al. (2014) (CPCAPE) with 45 lightning flashes s^{-1} (scale factor of 1.20 with the lowest global spatial correlation 0.388) underestimates tropical and midlatidude continental flash frequency, while it overestimates flash rates over the oceans as was also recently pointed out by Romps et al. (2018). The land (0.580)/ocean (0.278) spatial correlations of the CPCAPE parameterization are similar to those of the CP case.

The CTH-M lightning parameterization proposed by Michalon et al. (1999) is an improvement of the ocean flash rate with respect to the parameterization based on the convective CTH by Price and Rind (1992). Consequently, the land-ocean flash rate is more equilibrated with respect to the CTH parameterization (land/ocean spatial correlations of 0.718/0.684 for CTH-M vs. 0.726/0.756 for CTH) but both the tropical and midlatitude land flash rates are overestimated. The maritime flash rate is also overestimated. As a result of all this, the CTH-M parameterization by Michalon et al. (1999) produces a relatively high annual lightning rate of 51 flashes s^{-1} (scale factor of 1.61 with a high global spatial correlation of 0.712).

The updraft mass flux-based lightning parameterization (MFLUX) by Allen and Pickering (2002) produces 45 lightning flashes s^{-1} (scale factor of 1.80 with a global spatial correlation of 0.415), underestimates the midlatitude maritime and continental lightning flash rates in central Africa, south and central North America and India but, at the same time, overestimates it over many regions of Russia and the tropical ocean. The land (0.412)/ocean (0.431) spatial correlations of the MFLUX parameterization are also similar to those of the CP case.

Finally, the upward cloud ice flux-based (ICEFLUX) lightning parameterization slightly underestimates/overestimates the maritime/continental lightning flash rate producing 47 lightning flashes s^{-1} (scale factor of 4 with the highest global spatial correlation of 0.732). The ICEFLUX schemes exhibits the largest land and the second largest (slightly below CTH) ocean spatial correlations of 0.738 and 0.723, respectively. The reason why the overall (global) spatial correlation for ICEFLUX (0.732) exceeds that of CTH (0.729)—given that CTH ocean (0.756) exceeds ICEFLUX ocean (0.723)—is due to the fact that the correlation parameter (see caption of Table 1) depends on lightning counts, that is, higher counts over land than ocean so that land is more strongly weighted in the overall calculation.

Then, we found that ICEFLUX produces the largest global spatial correlation (0.732), while both CTH and CTH-M show almost the same global spatial correlations (0.712–0.729). This is because maritime flashes only represent 10% of the total number of flashes, and consequently, the maritime correction of the CTH-M

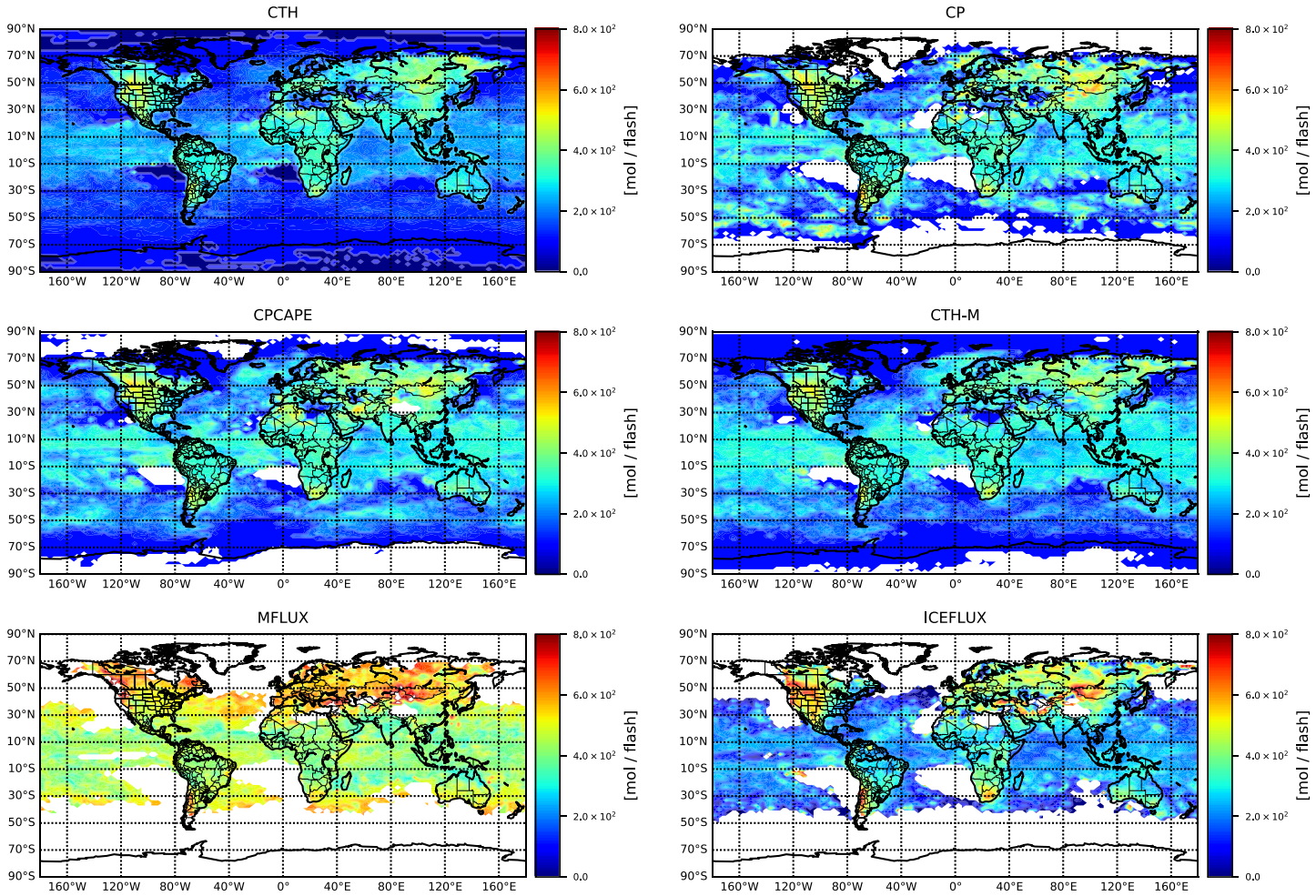

Figure 4. Predicted geographical distribution of lightning-produced NO_x in mol flash^{-1} for the six lightning schemes implemented in CAM5 correspoding to, respectively, the cloud top height (CTH) parameterization (Price & Rind, 1992), the convective precipitation (CP)-based parameterization (Allen & Pickering, 2002), the convective precipitation and CAPE (CPCAPE)-based parameterization (Romps et al., 2014), the lightning scheme by (Michalon et al., 1999) consisting in the CTH parameterization (Price & Rind, 1992), and an ocean flash rate upgrade (CTH-M) with respect to CTH, the updraft mass flux (MFLUX)-based parameterization (Allen & Pickering, 2002) and the upward cloud ice flux (ICEFLUX)-based parameterization (Finney et al., 2014). The spatial resolution is 2.5° longitude × 1.9° latitude.

with respect to CTH is hardly noticeable in r. The three other lightning parameterizations exhibit global r values between 0.388 (CPCAPE) and 0.448 (CP). The supporting information shows figures illustrating the appearance of the spatial distribution of each considered parameterization with respect to the observed distribution of OTD/LIS recordings. The global and land/ocean spatial correlations and the scale factors for the six lightning parameterizations investigated in this paper are shown in Table 1.

The left panel of Figure 3 shows a monthly global average for the six lightning parameterizations considered and OTD/LIS data. We see a 1-month backward shift (with respect to OTD/LIS data) of the CP, CPCAPE, and MFLUX lightning schemes, while the peak month of the lightning parameterizations based on the CTH, that is, CTH and CTH-M, is the same as that of the LIS data. The ICEFLUX parameterization is the only one exhibiting a 1 month forward shift with respect to LIS. An interesting feature of the MFLUX parameterization is that while it follows the OTD/LIS lightning frequency density, it slightly underestimates it during the spring-summer seasons (March through late September) and overestimates it during the fall-winter seasons (October through late February).

An interesting feature visible in the left panel of Figure 3, also reported by Tost et al. (2007) using the ECHAM5/MESSy model, is the double peak structure exhibited by most parameterizations. There is a secondary maximum during the Northern Hemisphere (NH) winter months when the lowest lightning rate

is observed. This causes that during the NH winter most ligthning schemes (except CTH and MFLUX) significantly overestimate the global average flash frequency. According to Tost et al. (2007) the NH winter maxima of most lightning schemes are due to overestimated oceanic flash occurrences in the tropics and the incorrectly captured displacement of regions with intense convection over the oceans. The latter led Tost et al. (2007) to conclude that lightning schemes that hardly distinguish between ocean and land flash parameterizations have problems to reproduce the observed lightning seasonal cycle. However, this conclusion does not completely apply to our simulations with CAM5. In our case, the CTH, CTH-M, and ICEFLUX schemes propose different parameterizations for the sea and land flash densities. However, only the CTH scheme (with the largest ocean spatial correlation as shown in Table 1) approximately reproduces the observed lightning annual seasonal cycle. Interestingly, the MFLUX scheme (with low ocean and land spatial correlations)—also used by Tost et al. (2007) in ECHAM5/MESSy with our same convection scheme—reproduces reasonably well in CAM5 the lightning monthly global average although it exhibits a consistent underestimate in the magnitude of the seasonal cycle.

The monthly tropical and midlatitude averages for the six tested schemes and the OTD/LIS data are represented in the right panel of Figure 3. This plot shows that the lightning flash rate density is larger in the tropics than in the midlatitudes. The tropical lightning frequency density exhibits a considerable smaller seasonal variation than the one of the midlatitude flash rate. Moreover, it is clearly visible that in January and December the tropical flash density of all tested schemes are overestimated (with respect to OTD/LIS), which explains the overestimation also exhibited in January and December by the global averaged flash rate density (see left panel of Figure 3).

3.1.2. Lightning-Produced NO_x

Figure 4 shows the predicted geographical distribution of lightning-produced NO_x (in mol flash^{-1}) for the six lightning schemes considered in our simulations. The general behavior shown in Figure 4 is that LNO_x in the midlatitude regions is between 6% and 40% larger than in the tropics (from 25°N to 25°S) for five of the lightning schemes explored except for CPCAPE. The obtained geographical distribution of LNO_x per flash is a consequence of the predicted geographical distribution of the IC/CG ratio. Other effects influencing the LNO_x per flash are out of the scope of this work (Price & Rind, 1993). This result is supported by a number of observations. During the TROCCINOX lightning campaign in 2004–2005, high NO_x per flash was observed over Florida, while tropical LNO_x production over Brazil was found to be lower (Huntrieser et al., 2007, 2008). In addition, the observational results by both Beirle et al. (2010) and Bucsela et al. (2010) are generally consistent with previous (Huntrieser et al., 2008) tropical estimates of lightning NO_x production rates and lower than rates at higher latitudes. Finally, in a recent American Meteorological Society presentation by Pickering et al. (2018) it was stated that (1) tropical analyses using OMI V3 data and improved tropospheric background and stratospheric NO_2 treatment give LNO_x production efficiencies estimates ranging from 47 ± 21 moles/flash over Africa to 149 ± 67 moles/flash over the tropical Pacific, with all tropics mean of 90 ± 36 moles/flash → 1.8 Tg N year^{-1}. (2) Midlatitude analysis yields a mean LNO_x production efficiencies of 320 ± 180 moles/flash, also using OMI V3 and updated background and stratosphere treatment → 6.4 Tg N year^{-1}. (3) Weighting these production rates by climatological flashes in tropics and midlatitudes (2/3 of flashes in tropics and 1/3 in midlatitudes in June–August), they obtain a global total LNO_x production of 4.4 ± 1.8 Tg N year^{-1}.

Table 2 shows the predicted total LNO_x per flash and the corresponding tropical and midlatitude LNO_x for each lightning scheme investigated together with the corresponding global spatial correlations in the tropical and midlatitude regions. CPCAPE has similar tropical (302 mol flash^{-1}) and midlatitude (300 mol flash^{-1}) LNO_x per flash values, while CTH exhibits a relatively small (8%) difference between tropical (312 mol flash^{-1}) and midlatitude (337 mol flash^{-1}) LNO_x per flash. However, ICEFLUX shows an important difference of ≃42% between tropical (288 mol flash^{-1}) and midlatitude LNO_x (406 mol flash^{-1}) values. Table 2 indicates that the ICEFLUX scheme presents: (1) The largest (well above CTH) midlatitude global spatial correlation (with respect to LIS/OTD observations) and (2) the second largest (after CTH) tropical spatial correlation. The predicted LNO_x geographical distribution can be better visualized in the map for ICEFLUX in Figure 4 where midlatitude continental regions exhibit larger (yellowish, reddish) LNO_x per flash than in the tropics (bluish, greenish).

The case of the MFLUX scheme in Figure 4 is different because, while there is a clear tropical region with smaller LNO_x per flash than in the midlatitude regions (as for ICEFLUX), the relative amount of IC lightning (with respect to CG lightning), which is the mean IC/CG ratio, is less (by approximately a factor of 2) than in

Table 2
Predicted Global, Tropical (From 25°N to 25°S) and Midlatitude Lightning-Produced NO_x (in mol $flash^{-1}$) and the Corresponding Tropical and Midlatitude Global Spatial Correlations

Lightning scheme	Predicted LNO_x (mol $flash^{-1}$)	Predicted tropical LNO_x (mol $flash^{-1}$)	Tropical spatial correlation global	Predicted midlatitude LNO_x (mol $flash^{-1}$)	Midlatitude Spatial correlation global
CTH[(1)]	328	312	0.766	337	0.553
CTH-M[(2)]	322	307	0.737	341	0.579
CP[(3)]	312	299	0.408	318	0.474
MFLUX[(4)]	441	404	0.368	476	0.542
CPCAPE[(5)]	302	302	0.284	300	0.618
ICEFLUX[(6)]	337	288	0.749	406	0.632

Note. The superscripts in the first column stand for the reference of the lightning scheme: (1) Price and Rind (1992), (2) Michalon et al. (1999), (3) and (4) Allen and Pickering (2002), (5) Romps et al. (2014), (6) Finney et al. (2014).

the rest of lightning schemes considered (see the mean IC/CG values shown in Table 1 for the six lightning schemes).

The mean IC/CG changes from a minimum of 2.15 (MFLUX) to a maximum of 4.24 (CPCAPE). The three parameterizations with the largest global spatial correlations exhibit mean IC/CG values varying in a narrow gap from 3.60 (ICEFLUX) to 3.80 (CTH) and 3.94 (CTH-M). The MFLUX scheme presents the least mean IC/CG ratio and, consequently, the largest LNO_x of 441 mol $flash^{-1}$ (see Table 1) due to the more relative abundance of CG lightning. The geographical distributions of the IC/CG for the six lightning schemes considered are shown in a figure in the supporting information. It is found that, in general, it is not straightforward to establish a latitudinal variation only of the IC/CG ratio. For additional information, the geographical distributions of the predicted cloud-to-ground (CG), intracloud (IC) lightning flash densities, and that of the geographical distribution of the IC fraction have also been included in the supporting information.

3.2. Annual Global Averaged Vertical Profiles

In this section we compare the impact of the six different lightning parameterizations implemented in CAM5 on different atmospheric chemical species. We have used the vertical distribution of LNO_x emissions recommended by Pickering et al. (1998), which suggested three different vertical profiles: midlatitude continental, tropical continental, and tropical marine. As the spatial distribution of lightning is different for each tested scheme, the vertical global averaged profile of the lightning NO production rate (shown in Figure 5) and the vertical global averaged profiles showing the chemical influence of lightning in the atmosphere (shown in Figure 6) depend on the considered lightning scheme.

The global average vertical profiles of the lightning NO production rates (these profiles are the ones injected in the chemical module of CAM5) for each lightning scheme are shown in Figure 5. There is an important variability up to ~2 km, then it stays relatively unchanged up to ~4 km when it starts to increase to reach a maximum injection in the troposphere between ~7.5 km and ~9 km depending on the lightning parameterization used. From ~10 km to ~16 km there is a monotonic decrease of more than six orders of magnitude.

Figure 6 includes a set of global average vertical profiles showing the influence of lightning on the concentration of NO, NO_2, trace species (CO, SO_2, O_3, and HNO_3) and hydrogen oxides (OH, HO_2, and H_2O_2) in the troposphere, upper troposphere (UT) and LS. Each panel of Figure 6 includes the species absolute concentration in the atmosphere with and without lightning together with the relative variation (in percentage) of the investigated chemical species with respect to their ambient concentrations in an atmosphere with no lightning. According to Figure 6 all parameterizations indicate that the influence of lightning on the densities of NO and NO_2 extends from ~2.5 km to ~19 km. For the CP, CPCAPE and MFLUX parameterizations there is a clear peak of the absolute NO density in the UT between ~15 km and ~16 km and a decreasing NO concentration from ~15 km to ~19 km. However, in contrast to the behavior of CP, CPCAPE, and MFLUX above ~11 km, it is worth noting that the parameterizations based on the upward ice flux at 440 hPa (ICEFLUX), CTH and maritime modified CTH-M exhibit an almost monotonic increase of the NO

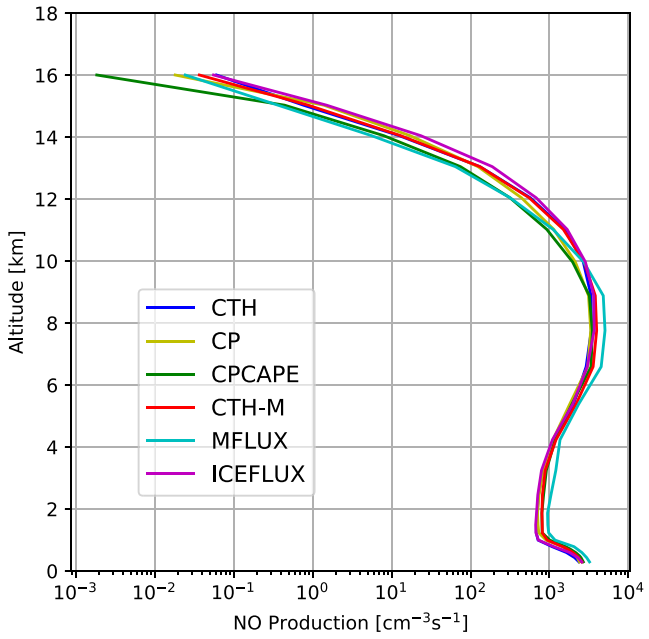

Figure 5. Vertical (geometric altitude) global averaged (90°S to 90°N) profiles showing the NO production rate due to the six lightning schemes considered. This NO lightning production rate is injected into the chemical module of CAM5 and produces variations in the density of different chemical species as shown in Figure 6.

concentration from ~12 km up to ~18 km where a very slight decreasing begins up to ~20 km. The altitude where the CP, CPCAPE, and MFLUX parameterizations place the maximum NO number density differs because it is conditioned by the relative importance (in each parameterization) of the three different (tropical continental/marine and midlatitude continental) vertical distribution profiles of the produced LNO_x.

The minimum absolute enhancements in NO and NO_2 appears in the lightning schemes based on, respectively, the upward ice flux at 440 hPa (ICEFLUX) for NO and the CPCAPE scheme for NO_2. However, the maximum absolute enhancements in NO and NO_2 are exhibited by the MFLUX (up to 12 km) and CP (from 12 km to 19 km) lightning parameterizations for NO and also by the MFLUX (up to 12 km) and CP (from 12 km to 19 km) schemes for NO_2. According to our calculations (see Table 1), the total annual global NO_x emission and flash frequency due to lightning ranges between 5.9 Tg N year^{-1} (and 44 flashes s^{-1}) for the CP parameterization and 8.5 Tg N year^{-1} (and 45 flashes s^{-1}) for the MFLUX parameterization.

According to the OTD/LIS lightning climatology used in this work, the global lightning flash frequency is 46 flashes s^{-1}, while the latest estimations of the global lightning NO_x emissions by new cloud-sliced observations of UT NO_2 in the 6- to 9-km range from the OMI satellite instrument points to a global NO_x yield of 280 moles per lightning flash and a global lightning NO_x source of 5.9 ± 1.7 Tg N year^{-1} for the year 2006 (Marais et al., 2018) within the consensus estimate of 5 ± 3 Tg N year^{-1} (Schumann & Huntrieser, 2007). The results by (Marais et al., 2018) do not support previous studies reporting higher lightning NO_x production rates in the midlatitudes than in the tropics (Nault et al., 2017; Schumann & Huntrieser, 2007). In this regard the recent results by (Nault et al., 2017) indicate a high production rate of ~9 Tg N year^{-1} with recommended values between ~370 mol NO flash^{-1} and ~670 mol NO flash^{-1} but with higher LNO_x production in the midlatitudes than in the tropical regions. Previous results obtained during the DC3 campaign in North America indicate lower lightning NO_x production in the range 117–332 mol NO_x flash^{-1} including uncertainties (Pollack et al., 2016). Our present study suggests that, when using CAM5, the ICEFLUX (closely followed by the CTH) lightning parameterization predicting 6.8 Tg N year^{-1}, 337 mol NO flash^{-1} and a global lightning frequency of 47 flashes s^{-1} is the one showing the largest global and midlatitude spatial correlation with respect to the global and midlatitude lightning frequency distribution observed by OTD/LIS.

In the following we explore the influence of tropospheric and lower stratospheric lightning-produced NO and NO_2 on the atmospheric chemistry by correlating the calculated NO and NO_2 with the predicted concentrations and behaviors of some trace gases and hydrogen oxides. When possible we also try to compare the obtained results with available results from measurements under lightning and/or thunderstorm conditions.

Our calculations indicate that lightning (through the production of NO_x) promotes an enhancement in the concentration of tropospheric ozone (O_3) that ranges between 32% and 45% with respect to ambient values with no lightning and with the maximum relative enhancement at ~7.5 km in agreement with modeling results by Finney et al. (2016). The calculated global average vertical profiles for O_3 follow the measured values (approximately doubles between ground level and 8 km) of different available observations (Martini et al., 2011). The analysis of the different lightning parameterizations indicates that the CTH parameterization produces the lowest relative increase in O_3 followed by CP and ICEFLUX while MFLUX and the maritime CTH modified (CTH-M) induce the highest relative increase.

The influence of the ICEFLUX and CTH lightning schemes on the tropospheric ozone chemistry was recently investigated by Finney et al. (2016) using the UKCA model coupled to the atmosphere-only version of the UK Met Office Unified Model 8.4. Finney et al. (2016) found that the ICEFLUX lightning scheme reduced the overestimation of tropical lightning caused by the CTH scheme resulting in less NO emission in the tropical upper troposphere and more in the extratropical regions. This causes a shift of the O_x (odd

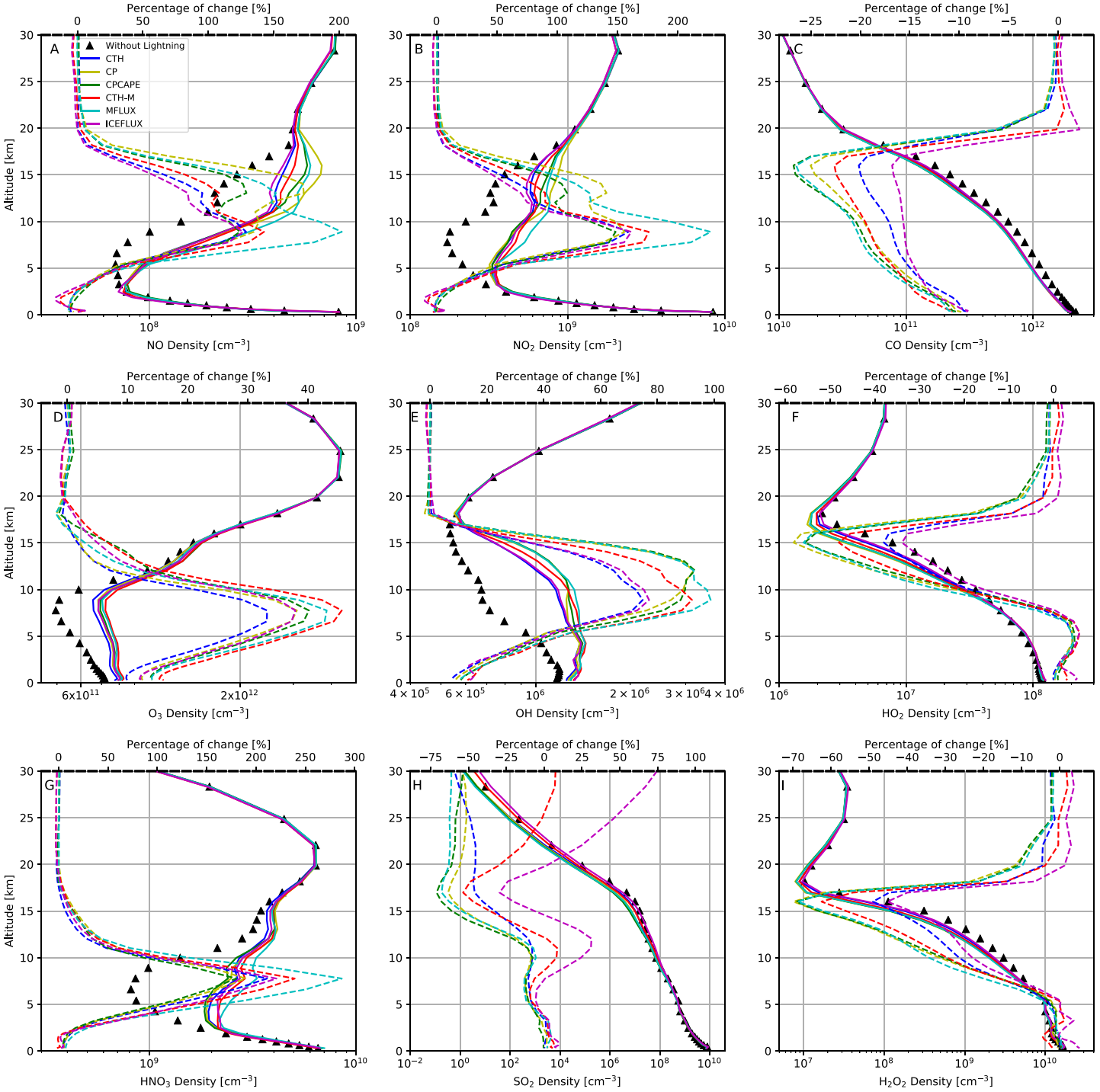

Figure 6. Vertical (geometric altitude) global average (90°S to 90°N) profiles showing the relative (dashed lines) and absolute (solid lines) lightning-induced variation in the density of key atmospheric chemical components such as nitrogen monoxide (NO), nitrogen dioxide (NO_2), carbon monoxide (CO), ozone (O_3), hydroxil radical (OH), hydroperoxyl radical (HO_2), nitric acid (HNO_3) and sulfur dioxide (SO_2), and hydrogen peroxide (H_2O_2). It is also shown for comparison the density of each chemical species in an atmosphere without lightning (triangles).

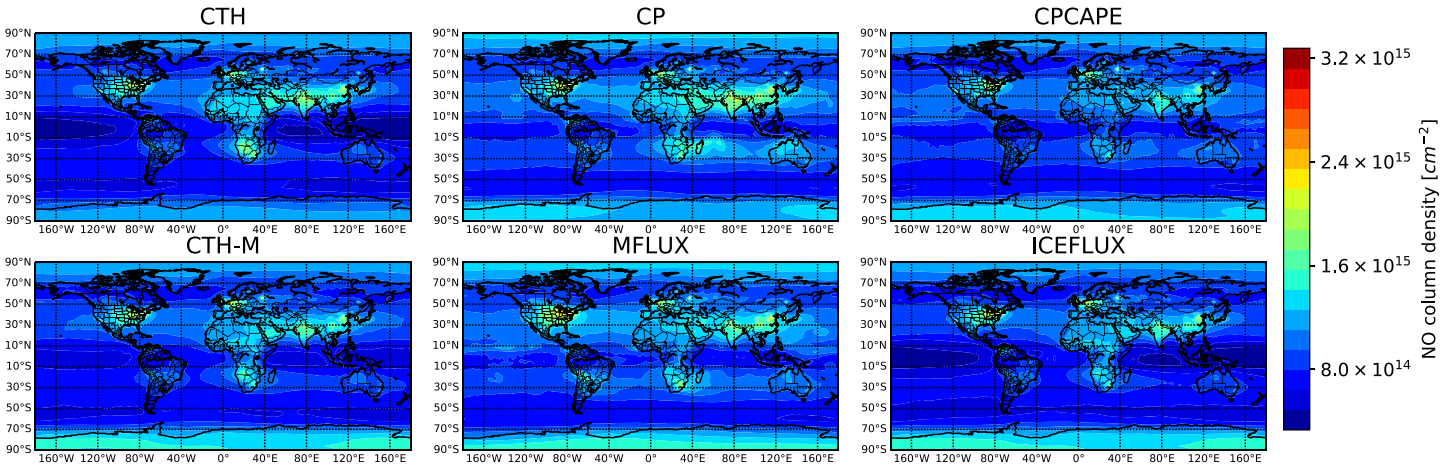

Figure 7. Total annual mean NO column density (from ground to 30 km) versus longitude and latitude for the six different lightning parameterizations implemented in CAM5 in this study.

oxygen species) production away from the upper tropical troposphere that results in a 5–10% reduction in upper tropical troposhere O_3 concentration along with smaller reductions in the LS and small increases in the extratropical troposphere (Finney et al., 2016). Therefore, the differences in the regional lightning distribution of the CTH scheme found by Finney et al. (2016) using the UKCA model increase O_3 in the upper tropical troposphere and, when compared with measurements by ozone sondes, reduces the correlation to observations in O_3 annual cycle in the tropics.

Nitric acid (HNO_3) (see Figure 6) is another interesting trace gas (connected to acid rain) in the atmosphere that is very sensitive to lightning and that, as O_3, is sensitive to the vertical placement of lightning NO_x emissions (Labrador et al., 2005). Our simulations indicate that the greatest absolute enhancement of HNO_3 with respect to background values without lightning is at ~7.5 km. The relative increase of HNO_3 ranges between 170% (for the CPCAPE parameterization) and about 300% (for the MFLUX parameterization). The formation of HNO_3 during daytime is promoted by the reaction of NO_2 with OH. During nighttime NO_2 converts to HNO_3 through the formation of N_2O_5 followed by heterogenous hydrolysis on aerosol particles. In agreement with measurements (Cooper et al., 2014; Martini et al., 2011) the variations of the calculated HNO_3 vertical profile is larger in the lower troposphere (<4 km) than in the UT/LS. We found that lightning-induced NO_x increases correlate with increases in HNO_3 but the maximum increase of HNO_3 due to lightning occurrs in the middle troposphere (7–10 km) while that of NO_x is in the UT (10–15 km).

Four out of six lightning parameterizations considered in this work (see Figure 6) indicate that the SO_2 number density is depleted and maintained almost unchanged from ~17 km to ~30 km. However, in the cases of the ICEFLUX and CTH-M parameterizations, the predicted lightning-driven SO_2 minima at ~17 km are followed by increasing SO_2 concentrations. The behavior of SO_2 can be due to the reaction $SO_2 + OH \rightarrow SO_4$. If one looks above 15 km in Figure 6 (E) for OH, slight negative (of about 1% or 2%) relative changes are visible for the CTH-M and ICEFLUX schemes. These small relative negative changes over an absolute OH density ranging between 10^5 and 10^6 cm^{-3} can promote significant relative increases of SO_2 (over a small absolute concentration between 1 cm^{-3} at 30 km and 10^4 cm^{-3} at 20 km) due to lightning activity. The opposite behavior for the CTH, MFLUX, CP, and CPCAPE schemes, that is, a small relative increase of the OH concentration (over a high absolute density) can also explain the depletion of SO_2 at high altitudes (above 15 km) due to chemical reaction with OH.

Regarding CO, our results indicate that when the amount of NO_x produced by lightning increases (when using different parameterizations) larger decreases in CO are obtained.

As can be seen in Figure 6, the influence of lightning on CO and SO_2 is, contrary to the case of O_3 and HNO_3, to decrease their concentrations with respect to their ambient values without the presence of lightning. The lowest absolute values and relative decrease (of up to 27%) for CO and (of up to 70%) for SO_2 are in the LS at, respectively, ~16 km and ~17 km with the particularity that the lightning depleted SO_2 concentration remains (except for ICEFLUX and CTH-M) between ~50% and ~60% below its background concentration

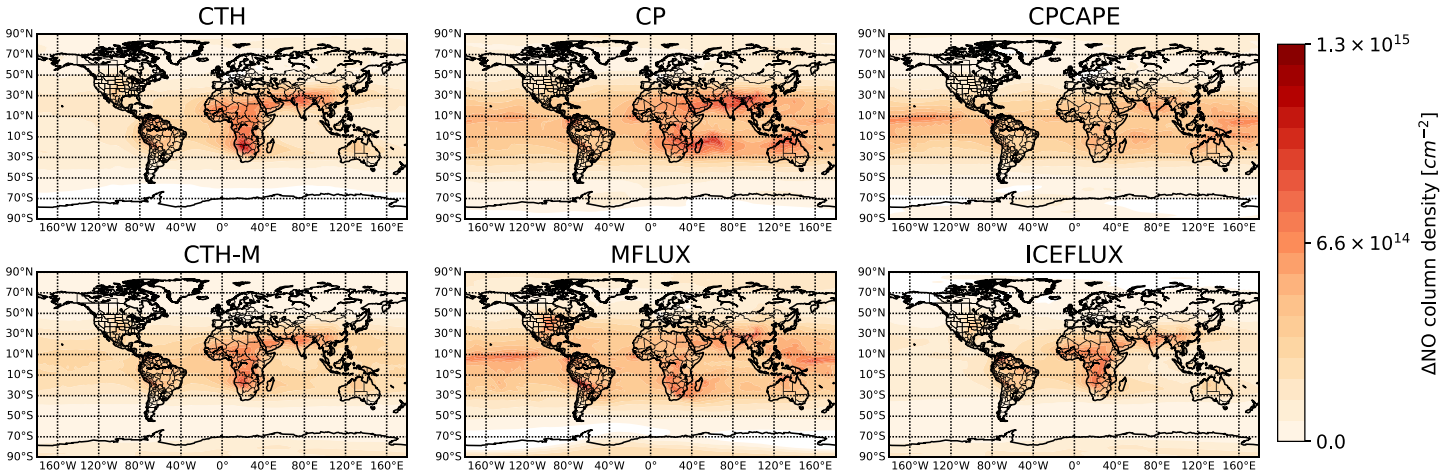

Figure 8. Enhancement due to lightning of NO column density (from ground to 30 km) versus longitude and latitude for the six different lightning parameterizations implemented in CAM5 in this study. The enhancement is calculated with respect to an atmosphere without lightning.

in an atmosphere with no lightning. The shape of the calculated global mean vertical profile for CO agrees reasonably well with aircraft measurements by Martini et al. (2011).

Lightning also influences the oxidizing capacity of the atmosphere by affecting the concentrations of hydrogen oxides (OH, HO_2, and H_2O_2) due to the lightning promoted enhancement of NO in the atmosphere. We have found that an increase in NO due to lightning produces enhancements of between ~75% and ~100%, depending on the parameterization used, in the OH density with a peak value at ~10 km. Lightning promotes the reaction of HO_2 with NO to produce OH and NO_2 that, globally, produces a depletion in the concentration of HO_2 that ranges between ~35% and ~60% with respect to ambient HO_2 values in an atmosphere without lightning that leads to a minimum in the density of HO_2 at ~15 km. For both OH and HO_2, the parameterizations based on the CTH and the upward ice flux-lightning relationship (ICEFLUX) produce the least impact while HO_2 is mostly affected by lightning parameterizations based on CP at the surface (only for precipitations stronger than 7 mm/day) (CP) and on the upward mass flux (MFLUX) and CPCAPE. Our calculations suggest that, in agreement with previous results by Labrador et al. (2004) and more recently by Liaskos et al. (2015), the relative variation in the vertical mean troposheric OH due to lightning more than doubles the relative variation in O_3.

The lightning promoted loss of H_2O_2 is due to the reaction of H_2O_2 with OH to produce H_2O and HO_2 that, globally, produces a depletion in the concentration of H_2O_2 that ranges between ~45% and ~70% with respect to ambient H_2O_2 values in an atmosphere without lightning and that leads to a minimum in the number density of H_2O_2 at ~16 km.

Finally, lightning promotes the oxidation of SO_2 by OH forming hydrogen sulfite (HSO_3) that reacts with atmospheric O_2 producing sulfur trioxide (SO_3) and HO_2. The reaction of SO_3 and water produces sulfuric acid (H_2SO_4) in the atmosphere. Consequently, the depletion of SO_2 by the influence of lightning (mediated by an increase of NO_x) promotes the generation of sulfuric acid in the atmosphere.

3.3. Annual Global Averaged Chemical Distribution

In the following we comment on the annual mean column densities of NO, NO_2, O_3, HNO_3, OH, HO_2, H_2O_2, CO, and SO_2 (from ground to 30 km) versus longitude and latitude as calculated for six different lightning parameterizations implemented in CAM5. The goal in this section is to compare between predictions of each of the parameterizations used and, when possible, to establish comparisons with available measured concentrations of lightning affected trace species at a global or regional level.

Our calculations for the global mean NO column density shown in longitude-latitude maps (see Figure 7) predict NO column densities of up to ~3×10^{15} cm^{-2} with clear hot spots (very active NO source regions) above latitude >30°N corresponding to highly polluted land regions. The south of Africa also exhibits relatively high NO column densities that are mostly connected to lightning activity in that region (see Figure 8 where only NO density enhancements resulting from the difference between simulations with and without lightning are shown).

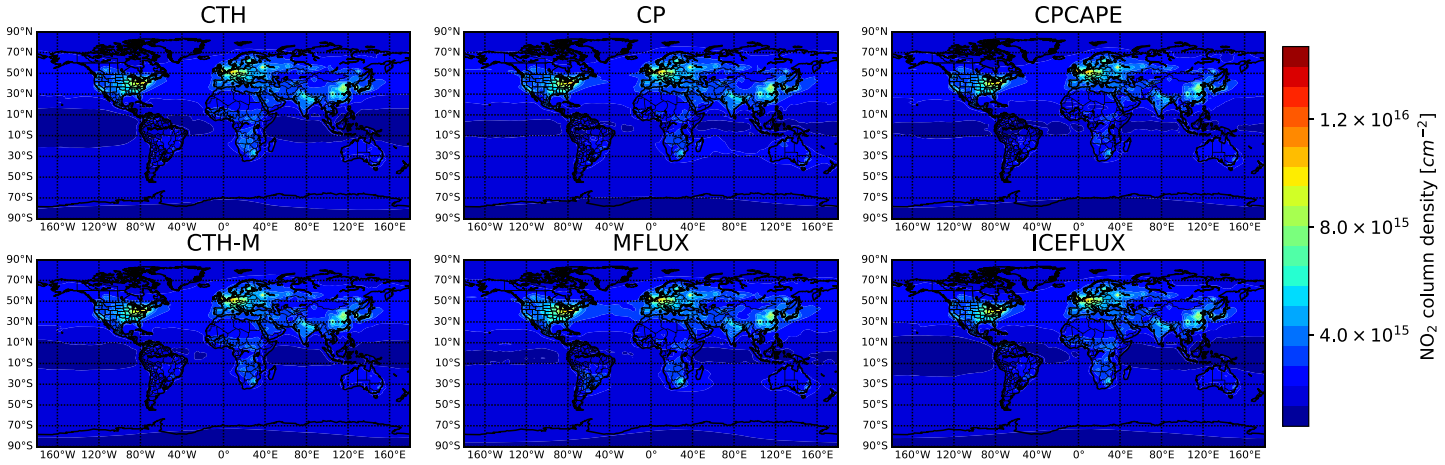

Figure 9. Total annual mean NO_2 column density (from ground to 30 km) versus longitude and latitude for the six different lightning parameterizations implemented in CAM5 in this study.

The lightning enhanced NO column densities shown in Figure 8 are mostly located within ±30° latitude with some small NO enhancement due to transport of lightning-produced NO also visible in the north and south polar regions. Depending on the lightning parameterization used in CAM5, the LNO_x contribution to the NO column can be of up to 1.3×10^{15} cm^{-2} in central and South Africa. The MFLUX parameterization predicts the highest NO enhancement (8.5 Tg N $year^{-1}$ and 441 mol $flash^{-1}$) due to lightning (see Table 1) but its global spatial correlation (with respect to OTD/LIS observations) is of only 0.415 and exhibits a lower land (0.412) than ocean (0.431) spatial correlations. The ICEFLUX followed by the CTH lightning parameterizations are the ones with the highest global (0.732) and land/ocean (0.738/0.723) spatial correlations and, therefore, their geographical distributions of enhanced NO due to lightning are the most reliable.

Our calculated global NO_2 column densities shown in Figure 9 agree with available measurements by GOME (Richter et al., 2005; Schumann & Huntrieser, 2007) showing similar quantitative values and global distribution of NO_2 with high NO_2 contaminated areas in the northeastern China, center northeastern United States, and central and northern Europe due to anthropogenic sources. According to our results, lightning can contribute up to ~2.5×10^{15} cm^{-2} NO_2 column density (15% of the maximum NO_2 column up to 30 km) as can be seen in Figure 10 and where lightning enhanced NO_2 is mostly visible in the ±30° region with maximum values in central and South Africa. In the case of North and South America, the CP and CPCAPE schemes predict the lowest lightning NO_2 enhancement among the six lightning schemes compared. The CTH, CTH-M and ICEFLUX schemes (with clear distinction between sea and land flash densities) predict

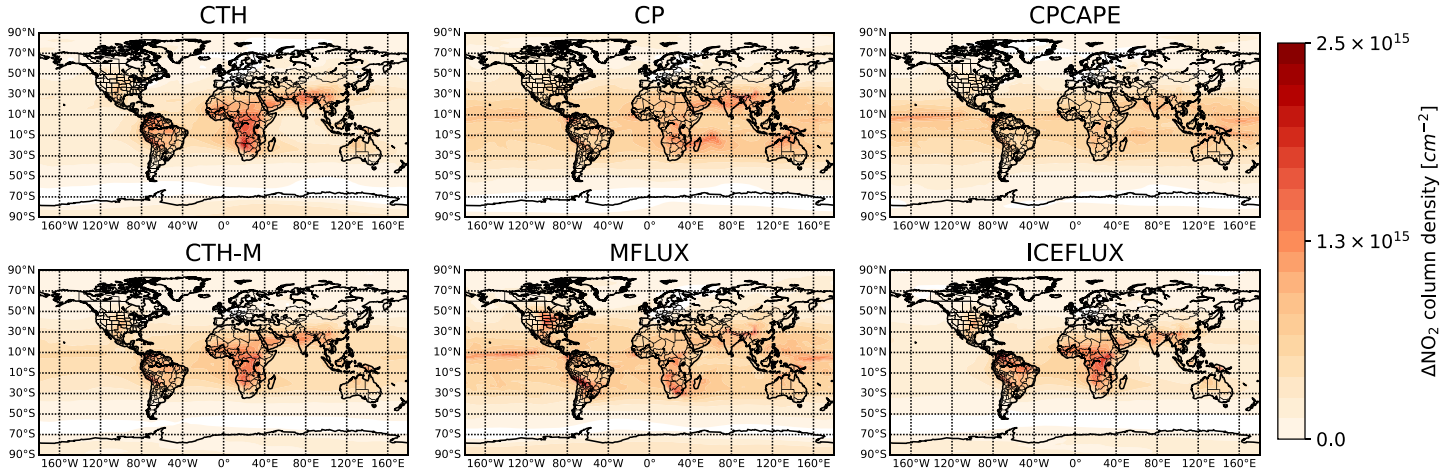

Figure 10. Enhancement due to lightning of NO_2 column density (from ground to 30 km) versus longitude and latitude for the six different lightning parameterizations implemented in CAM5 in this study. The enhancement is calculated with respect to an atmosphere without lightning.

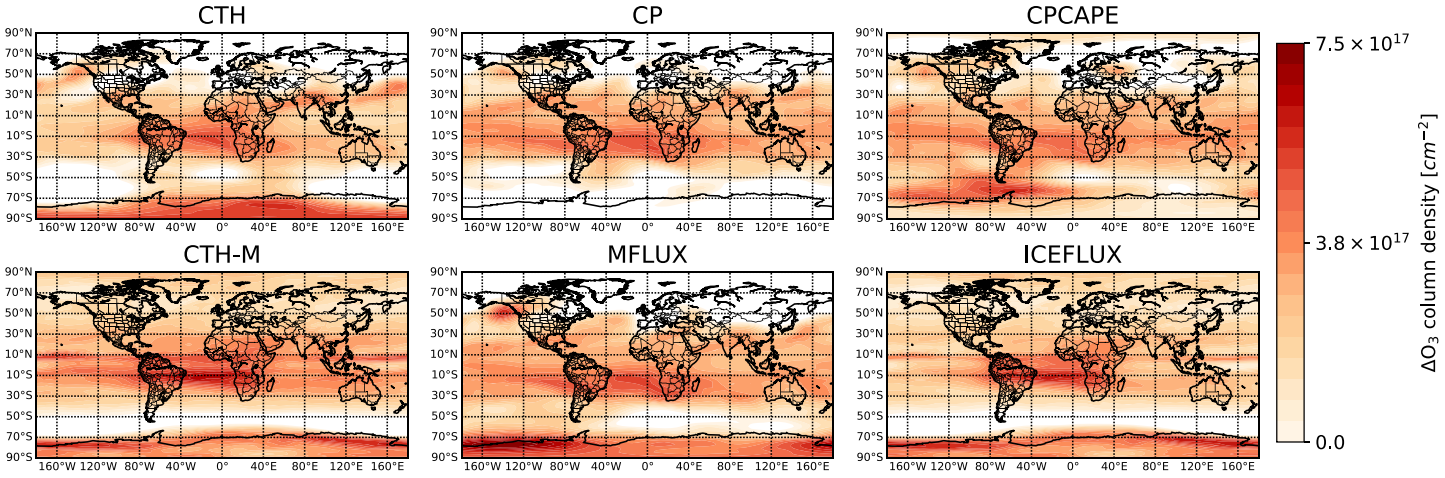

Figure 11. Enhancement due to lightning of O_3 column density (from ground to 30 km) versus longitude and latitude for the six different lightning parameterizations implemented in CAM5 in this study. The enhancement is calculated with respect to an atmosphere without lightning.

more lightning enhanced NO_2 in South America than the other tested schemes. These three schemes (CTH, CTH-M, and ICEFLUX) also predict significant NO_2 due to lightning in the Amazonia region where the three of them predict important lightning flash densities. Finally, the MFLUX parameterization predicts important NO_2 enhancement due to lightning in the eastern region of North America and central part of South America. As in the case of NO, there is also some slight NO_2 enhancement due to lightning in the northern (>50°N) and southern (>70°S) latitudes.

The predicted enhancement of O_3 due to lightning is shown in Figure 11 where it is clearly visible that lightning enhanced O_3 is mainly located in the tropical and subtropical regions where lightning produces more NO and NO_2. Five (except CP) of the six lightning parameterizations implemented in CAM5 predict a significant enhancement of O_3 due to lightning in the south polar regions. The CP scheme exhibits very weak O_3 lightning enhancement in the southern hemispheric oceanic areas so that O_3 transport from the nearby oceans is neglected in the CP scheme. This can explain the lack of lightning enhanced O_3 in the CP south polar regions.

In addition, the CP, MFLUX, and CTH parameterizations exhibit no lightning enhanced O_3 over 70°N. The CTH- and CPCAPE-based (but much less pronounced than CTH) lightning parameterizations predict an increase of O_3 in the Antartic regions with no equivalent NO enhancements. This could be related to ozone transported from the African and South American continents. Lightning parameterizations like CPCAPE,

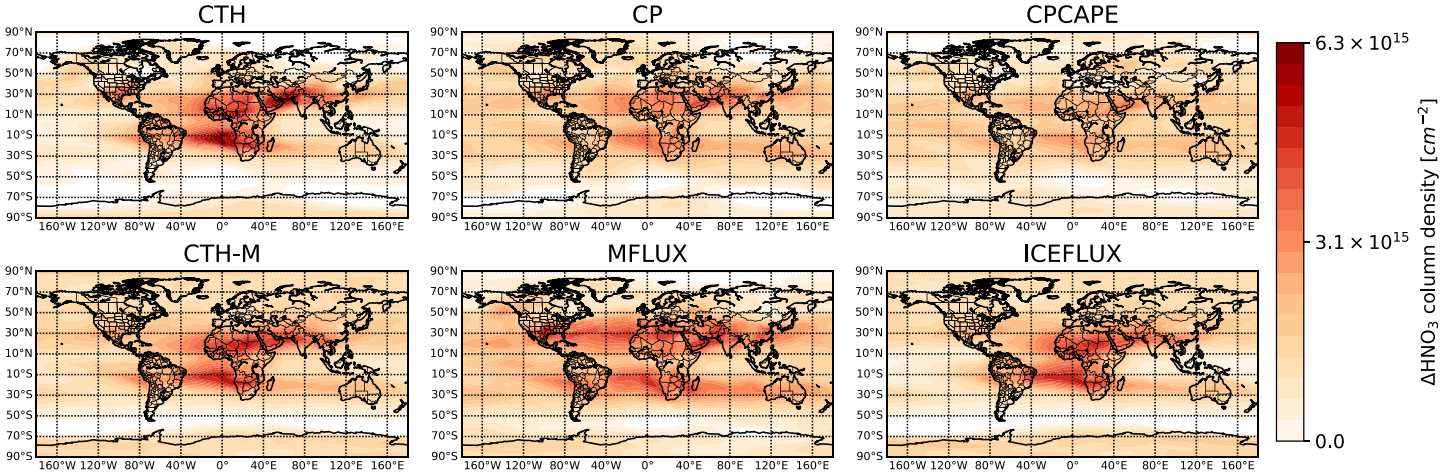

Figure 12. Enhancement due to lightning of HNO_3 column density (from ground to 30 km) versus longitude and latitude for the six different lightning parameterizations implemented in CAM5 in this study. The enhancement is calculated with respect to an atmosphere without lightning.

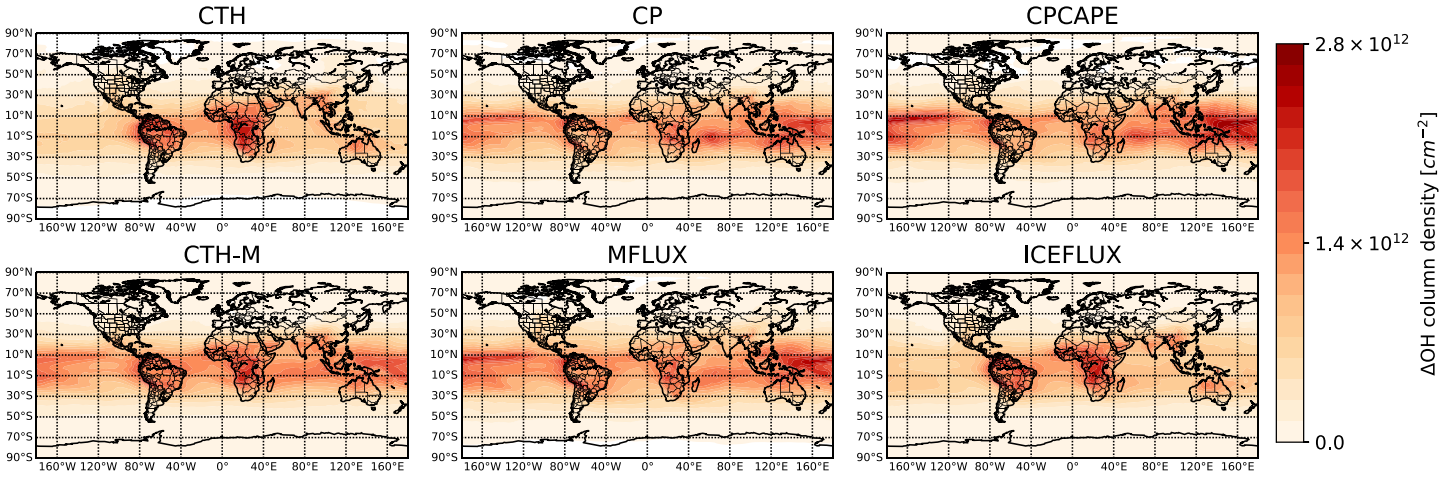

Figure 13. Enhancement due to lightning of OH column density (from ground to 30 km) versus longitude and latitude for the six different lightning parameterizations implemented in CAM5 in this study. The enhancement is calculated with respect to an atmosphere without lightning.

MFLUX, and CTH-M predict high O_3 increases in the maritime regions. All the parameterizations show nonnegligible O_3 increase at ∼10°S over the Atlantic Ocean where lightning density and NO enhancement are small (with respect to the maxima in central Africa). This might be connected to advection of tropospheric ozone and precursors from intense lightning regions of Africa (in the lower and middle troposphere) and South America (in the upper troposhere) (Finney et al., 2016; Grewe, 2007; Murray, 2016). According to our CAM5 simulations, lightning can contribute between ∼5% and ∼20% (or between 5 and 30 Dobson units) to the global ambient O_3 column. The least O_3 lightning enhancement is predicted by the parameterizations based on, respectively, the CTH followed by the CP and the upward ice flux at 440 hPa (ICEFLUX). The highest O_3 lightning enhancement is predicted by the CTH-M scheme.

The lightning enhanced HNO_3 (see Figure 12) can contribute to up to 25% to the HNO_3 column with hot spots in regions where lightning enhanced NO and NO_2 is important since the oxidation of NO_x by OH to nitric acid is a dominant sink of NO_x. The nonnegligible presence of lightning generated HNO_3 visible in Figure 12 at ∼10°S over the Atlantic ocean does not seem to be correlated to lightning flashes in that region but may be due to transport phenomena.

According to our simulations, the global concentration of OH is largely affected by lightning as can be seen in Figure 13. The production of OH in the atmosphere is initiated by the photolysis of O_3 that produces electronically excited oxygen atoms $O(^1D)$ that, after reacting with water vapor, generates OH molecules (Voulgarakis et al., 2013). Lightning promotes the formation of OH by oxidative reactions of lightning-produced NO with HO_2. All considered lightning parameterizations predict that lightning enhanced OH is mainly generated through the tropical and midlatitude regions between ±30° latitude. However, there are differences in the geographical distribution of lightning-produced OH depending on the parameterization used. The CTH-based and CTH-M-based parameterizations locate the OH due to lightning in Africa, India, southeastern Asia, and central South America. When parameterizations based on precipitation (CP) and convective available potential energy (CPCAPE) are used, lightning-produced OH is still important in Africa but it is mostly concentrated in southeastern Asia. When lightning is parameterized following the upward ice flux (ICEFLUX) and the CTH, we see that maritime regions become less active in lightning production of OH so that the lightning enhanced OH column density is the smallest in comparison with the other four considered parameterizations.

The effect of lightning on the column density of the hydroperoxyl radical (HO_2) is interesting since, as seen in Figure 14, there are continental regions (central Africa, Micronesia, and the northwestern of South America) where lightning promotes the local formation of HO_2 (due to the presence of high concentrations of lightning-produced OH reacting with O_3), while in other large land and oceanic regions HO_2 is depleted. All lightning parameterizations used in this study predict an overall depletion of the HO_2 column density caused by lightning within latitudes ±50°. The depletion of HO_2 caused by lightning could be promoted by chemical reactions driven by lightning-produced NO and NO_2 through $NO + HO_2 \rightarrow NO_2 + OH$ and

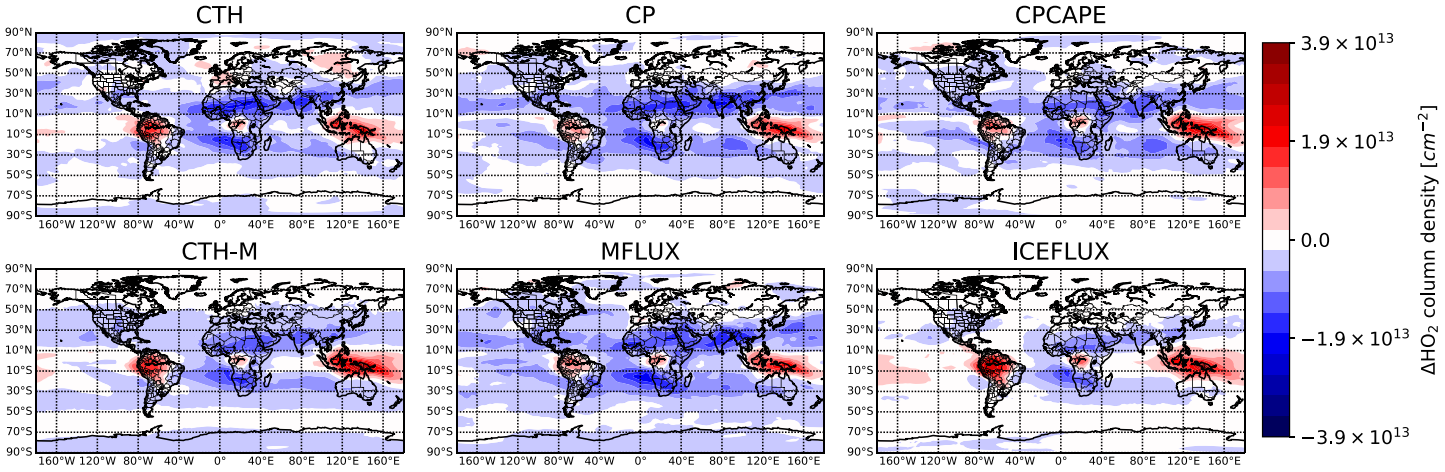

Figure 14. Enhancement due to lightning of HO_2 column density (from ground to 30 km) versus longitude and latitude for the six different lightning parameterizations implemented in CAM5 in this study. The enhancement is calculated with respect to an atmosphere without lightning.

$NO_2 + HO_2 + M \rightarrow HO_2NO_2 + M$ (promoted near the surface). A possible mechanism explaining lightning enhancement of HO_2 is the reaction of lightning generated O_3 with OH to produce HO_2 and O_2. The regions with HO_2 enhancements are around the Melanesia and in the north part of southern America close to Central America where there is considerable lightning activity.

The effect of lightning on the column density of hydrogen peroxide (H_2O_2) is also interesting since, as seen in Figure 15, there are regions in Micronesia, parts of South America (except for MFLUX and CPCAPE), Europe (only for CTH, CP, and MFLUX), and regions above ~50°N (for CTH, CP and CPCAPE) where lightning promotes the local formation of H_2O_2 by $HO_2 + HO_2 \rightarrow H_2O_2 + O_2$. In other large land and oceanic regions H_2O_2 is depleted due to lightning through its photolysis and by its interaction with OH ($H_2O_2 + OH \rightarrow HO_2 + H_2O$).

The way lightning influences on HO_2 and H_2O_2 changes from land to ocean because the vertical injection profiles of lightning-produced NO are also different over land and over the oceans. According to the employed vertical distribution of LNO_x recommended by Pickering et al. (1998), the injection of NO by lightning near the surface (between ground and ≃1.5 km of altitude) is greater over land than over the ocean. Therefore, the three-body reaction $NO_2 + HO_2 + M \rightarrow HO_2NO_2 + M$ that contributes to deplete HO_2 is more important in the case of LNO_x over land.

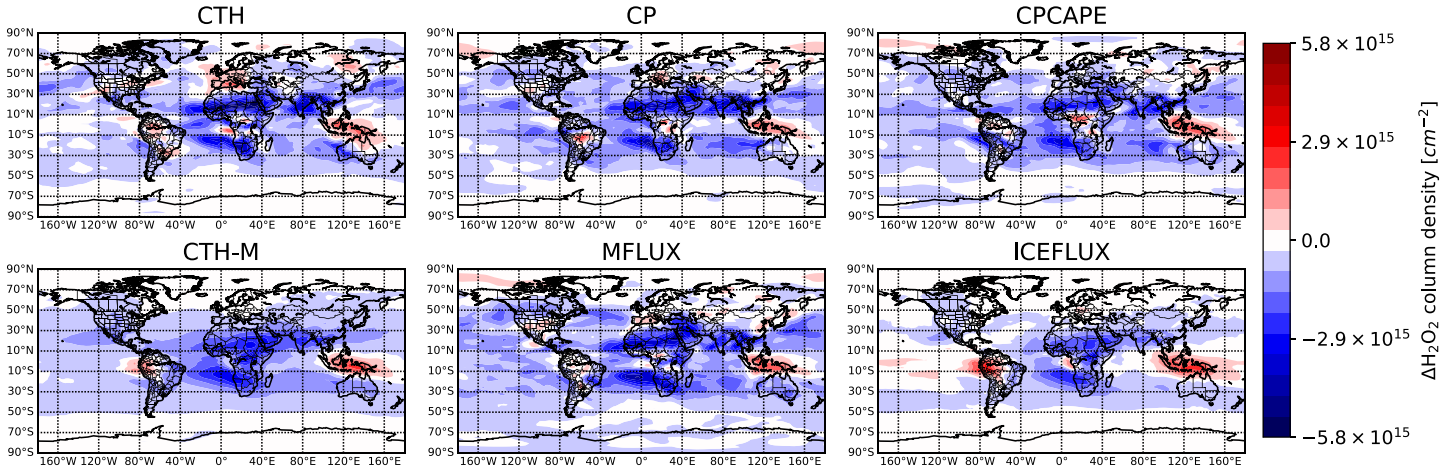

Figure 15. Enhancement due to lightning of H_2O_2 column density (from ground to 30 km) versus longitude and latitude for the six different lightning parameterizations implemented in CAM5 in this study. The enhancement is calculated with respect to an atmosphere without lightning.

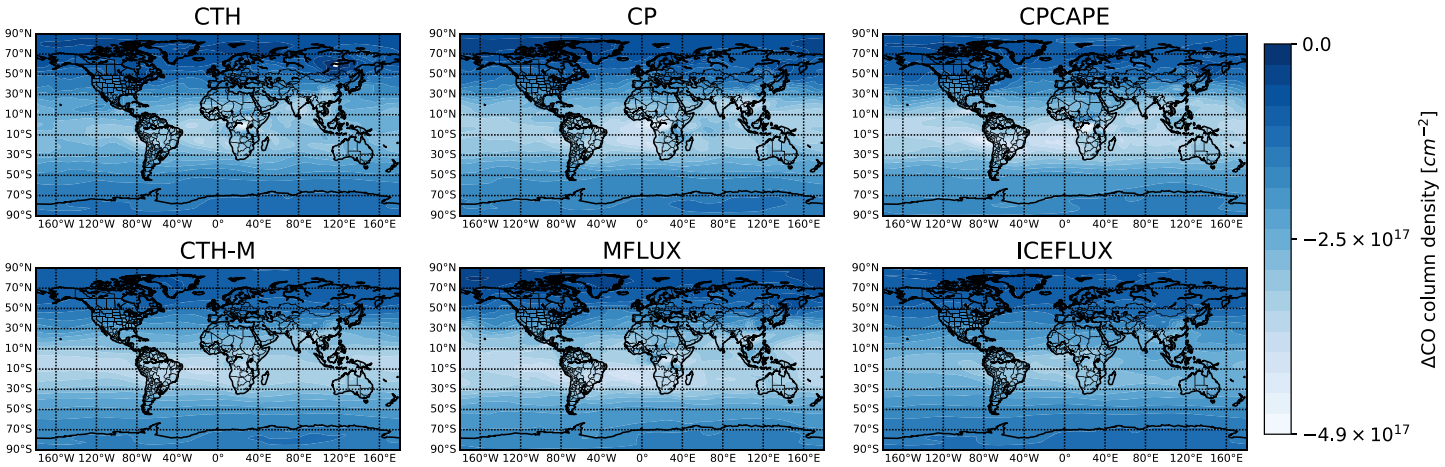

Figure 16. Enhancement due to lightning of CO column density (from ground to 30 km) versus longitude and latitude for the six different lightning parameterizations implemented in CAM5 in this study. The enhancement is calculated with respect to an atmosphere without lightning.

The presence of lightning (and lightning generated NO) produces a depletion in the concentration of CO (see Figure 16) that expands through the tropical regions. All tested lightning parameterizations produce the same NO-CO relationship with the MFLUX (and CPCAPE) parameterization predicting the largest CO depletion, while the ICEFLUX scheme predicts the lowest CO decrease mainly located in the tropical regions around 10°S. This behavior could be a consequence of the influence of OH on the lifetime of CO in the troposphere (Logan et al., 1981). Therefore, the larger the amount of lightning-produced OH the greater the depletion of CO due to oxidizing reactions such as $CO + OH + M \rightarrow CO_2 + HO_2 + M$ or $CO + OH \rightarrow CO_2 + H$. The MFLUX and ICEFLUX lightning schemes produce the largest and lowest OH enhancements, respectively.

There have been reports for the last 25 years suggesting that air highly polluted with SO_2 can promote cloud-to-ground lightning flashes due to increased sulfate aerosol (Kar et al., 2007; Orville et al., 2001; Soriano & de Pablo, 2002; Steiger et al., 2002; Westcott, 1995). In addition, global average SO_2 space-based observations by GOME between 1996 and 2002 (Khokhar et al., 2005) indicate that the main sources of atmospheric SO_2 emissions are biomass burning in some regions of Africa and the Amazonia, volcanic eruptions (Mount Nyiragongo in central Africa, Mount Etna in Sicily, and volcanoes of The Ring of Fire around the edges of the Pacific Ocean) and massively polluted urban and industrial areas (Beijing region, eastern Europe, northeastern of the United States, and the heavy mining industry region around the city of Norilsk above the Artic Circle in Russia).

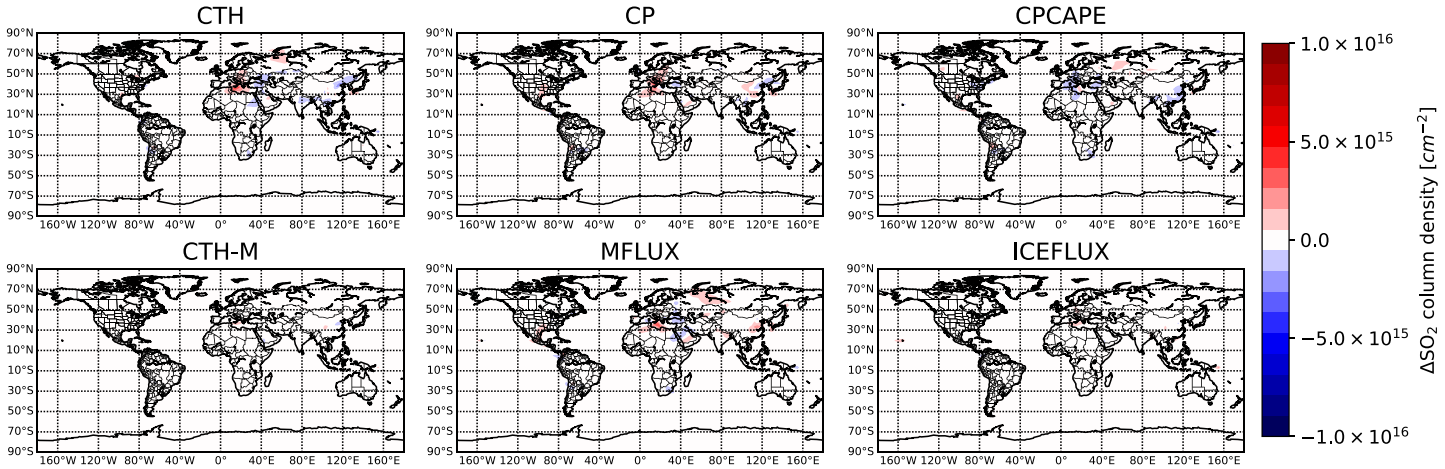

Figure 17. Enhancement due to lightning of SO_2 column density (from ground to 30 km) versus longitude and latitude for the six different lightning parameterizations implemented in CAM5 in this study. The enhancement is calculated with respect to an atmosphere without lightning.

According to Figure 17, all lightning parameterizations (especially CTH, CP, MFLUX, and CPCAPE) predict an enhanced lightning-driven SO_2 column density in regions relatively close to the sea with volcanic eruptions like the Mount Etna region, South America (80–40°W, 10–30°S) and the south of Japan. Some parameterizations (CTH, MFLUX, and CPCAPE and CTH-M) indicate minor SO_2 depletion in eastern Europe and close to the Beijing area (not for MFLUX) (120°E, 40°N) where the total ambient SO_2 column reaches its peak (see figure in the supporting information). Our explanation to these results is connected to the presence of dimethyl sulfide (DMS; an organic compound produced by oceanic plankton) in the sea and coastal regions that when reacting with lightning-produced OH would generate SO_2 through DMS + OH → SO_2 and DMS + OH → 0.5 SO_2 + 0.5 HO_2. Inside the continents, where the amount of DMS is negligible, the lightning generated OH would destroy SO_2 through SO_2 + OH → SO_4. These mechanisms could explain the lightning SO_2 production and depletion visible in the maritime (and coastal) regions and in continental regions of Figure 17, respectively.

4. Summary and Conclusions

The six different lightning parameterizations implemented in CAM5 extend from the surface up to ~40 km. Our CAM5 simulations cover a "present-day" year using climatological sea surface temperatures computed over monthly averages between the year 1982 and 2001. We have used lightning parameterizations based on the CTH by Price and Rind (1992), maritime upgraded CTH or CTH-M by Michalon et al. (1999), CP at the surface (for precipitations stronger than 7 mm/day) and on upward mass flux (MFLUX) at 440 hPa both proposed by Allen and Pickering (2002). Another lightning parameterizations used here are based on a combination of CPCAPE by Romps et al. (2014) and on upward ice flux at 440 hPa (ICEFLUX) by Finney et al. (2014). We have used scale factors to match the global lightning frequency (in flashes per minute) resulting from each of the lightning schemes considered to the global lightning frequency observed by OTD/LIS.

The six lightning schemes implemented in CAM5 can be divided into two groups according to their *r* values (see Table 1). The *low r* group formed by CPCAPE, MFLUX, and CP with *r* ranging between 0.388 (CPCAPE) and 0.448 (CP), and the *high r* group with CTH-M, CTH, and ICEFLUX with global spatial correlations between 0.712 (CTH-M) and 0.732 (ICEFLUX). In addition to the global spatial correlations, we have also calculated the corresponding land/ocean spatial correlations for each parameterization. We found that the *low r* group exhibit a relatively high land *r* (between 0.412 for MFLUX and 0.58 for CPCAPE) but shows low ocean *r* (below 0.431 for the three of them). As for the *high r* lightning parameterization group, all of them (especially ICEFLUX) reproduce—with a high degree of fidelity (land and ocean *r* above 0.73 and 0.72, respectively)—the lightning geographical distribution over the continents and oceans.

We have quantified the influence of the different considered lightning parameterizations on the densities of NO and NO_2 in the troposphere and LS but also on important atmospheric trace gases affected by lightning activity such as O_3, CO, HNO_3, SO_2, and the hydrogen oxides OH, HO_2, and hydrogen peroxide (H_2O_2). The lightning NO production rate is also evaluated. The fact that there are no global (only regional) measurements of lightning enhanced NO or NO_2 densities complicates comparison with model simulations. Thus, it is usually more convenient to compare with measured vertical profiles, since depending on region most UT-NO can be attributed to lightning production (at least in remote regions). However, we have compared predictions among lightning parameterizations and found that, for all parameterizations, the vertical global average densities of HO_2, H_2O_2, CO, and SO_2 are depleted due to lightning, while those of NO, NO_2, O_3, OH, and HNO_3 increase. The enhancements of NO and NO_2 due to lightning vary between minima of, respectively, 125% (for ICEFLUX) and 150% (for CPCAPE), and maxima of, respectively, >200% and >220% for MFLUX. The *low r* group of lightning parameterizations (CP, CPCAPE, and MFLUX) exhibit a clear peak of the absolute NO density in the UT between ~15 km and ~16 km and a decreasing NO concentration from ~15 km to ~19 km resembling measurements from the CRYSTAL-FACE 2002 thunderstorm experiment shown in Figure 4c in Huntrieser et al. (2016a). However, in contrast to this, the *high r* group of lightning parameterizations (ICEFLUX, CTH, and CTH-M) show an almost monotonic increase of the NO concentration from ~10 km up to ~18 km where a slight decreasing begins up to ~20 km. This might suggest that the predicted IC/CG ratio for *high r* parameterizations is likely problematic. The implementation of the IC/CG ratio in GCMs needs further investigation and improvements.

The predicted lightning-produced NO_x (averaged over all flashes) varies between a minimum of 310 mol $flash^{-1}$ (and 6 Tg N $year^{-1}$) for the CPCAPE parameterization and a maximum of 441 mol $flash^{-1}$ (and 8.5

Tg N year^{-1}) for MFLUX. There are intermediate scenarios like the ones predicted by the CP and ICEFLUX lighning parameterizations with, respectively, 312 mol flash^{-1}, 5.9 Tg N year^{-1} and 337 mol flash^{-1}, 6.8 Tg N year^{-1}. All (except that of MFLUX) these lightning-produced NO_x amounts are within the consensus estimate of 5 ± 3 Tg N year^{-1} (Schumann & Huntrieser, 2007). The differences in the LNO_x averages stem from the differences in the mean IC/CG flash ratios (see Table 1) between implemented lightning schemes, which result from differences in cold cloud depths.

Our study provides annual global distributions showing predictions for total (up to 30 km) column densities of NO, NO_2, and the trace gases mentioned before but also the specific contribution of lightning to the column density. It is in general very difficult to measure how lightning contributes to the column density of NO, NO_2, and other key chemical components of the atmosphere (Pickering et al., 2016). However, our results agree with the enhancement of NO_2 produced by lightning over tropical Atlantic and Africa as reported by Martin et al. (2007) where it is suggested the regions where column NO_2 measurements are likely dominated by lightning.

With respect to the investigated influence of lightning on traces gases, our results suggest that all parameterizations show nonnegligible O_3 increase at ~10°S over the Atlantic ocean where lightning density and NO enhancement are relatively small (with respect to the maxima in central Africa) but where advection of tropospheric ozone and precursors from intense lightning regions of Africa and South America can be important. According to our CAM5 simulations, lightning can contribute between ~5% and ~20% (depending on the regions) to the total global ambient O_3 column density and with the CTH and MFLUX schemes (in order of importance) being the parameterizations that produce the least O_3 lightning enhancement.

Lightning can also contribute to the formation of atmospheric acids such as HNO_3. In particular, lightning can be responsible for up to 25% of the total HNO_3 column density with very active regions where lightning enhanced NO and NO_2 is important since the oxidation of NO_x by OH to nitric acid is a dominant sink of NO_x and, consequently, limits the lifetime of NO_x. The important presence of lightning generated O_3 and HNO_3 at ~10°S over the Atlantic ocean could be due to transported lightning-produced NO_x.

Apart from lightning NO_x and ozone, the efficiency of lightning injected NO molecules to produce ozone depends on the availability of HO_x radicals and the lifetime of NO_x. A limiting factor for the lifetime of NO_x in the free troposphere is the conversion of NO_2 into HNO_3, which is soluble and can be eliminated by precipitating clouds. Therefore, the analysis and quantification of lightning-induced production of OH, HO_2, H_2O_2, and HNO_3 and how they interact with NO and NO_2 are important for the production of ozone.

Lightning promotes the formation of OH by oxidative reactions of lightning-produced NO with HO_2. All considered lightning parameterizations predict that lightning enhanced OH is mainly generated through the tropical and midlatitude regions between ±30° latitude. However, there are differences in the geographical distribution of lightning-produced OH depending on the parameterization used. When the ICEFLUX and CTH schemes are used, we see that the maritime regions become less active in lightning production of OH than the other four considered parameterizations.

The effect of lightning on the column density of the hydroperoxyl radical (HO_2) and hydrogen peroxide (H_2O_2) is interesting since there are continental regions where they are depleted by the action of lightning through $NO + HO_2 \rightarrow NO_2 + OH$, $NO_2 + HO_2 + M \rightarrow HO_2NO_2 + M$ (promoted near the surface) and through the photolysis of H_2O_2 and by its interaction with OH ($H_2O_2 + OH \rightarrow HO_2 + H_2O$). However, in other large land and oceanic regions HO_2 and H_2O_2 are promoted by the action of lightning generated O_3 with OH to produce HO_2 and O_2 and by the reaction $HO_2 + HO_2 \rightarrow H_2O_2 + O_2$.

Our simulations predict that the presence of lightning produces a depletion in the concentration of CO—as a consequence of the influence of lightning-produced OH on the lifetime of CO in the troposphere—that expands through the tropical regions and that is maximum and minimum when using the MFLUX and ICEFLUX schemes, respectively.

All used lightning schemes (especially CTH, CP, MFLUX, and CPCAPE) predict an enhanced lightning-driven SO_2 column density in regions relatively close to the sea with volcanic eruptions like the Mount Etna region, South America (80–40°W, 10–30°S) and the south of Japan. The presence of DMS (an organic compound produced by oceanic plankton) in the sea and coastal regions can react with lightning-produced OH generating SO_2 through $DMS + OH \rightarrow SO_2$ and $DMS + OH \rightarrow 0.5\ SO_2 + 0.5\ HO_2$.

Table 3
Indication—Based on the Six Lightning Schemes Investigated With CAM5—of the Geographical Regions of the World Where an Increase/Decrease of the Concentrations of NO, NO_2, O_3, OH, and HO_2 Is Expected Due to Lightning

Geographical Region	NO	NO_2	O_3	OH	HO_2
North Africa	+++	+++	+++	+++	−
Central Africa	++++	++++	++++	++++	+
South Africa	+++	+++	+++	+++	−
North-Eastern America	++	++	++	++	−
Gulf of Mexico	++	++	++	+++	−
Central America (10°N to 20°N)	++++	++++	++++	+++	+
South America (>30°S to 10°N)	+++	+++	++++	++++	+++
North Europe (>45°N)	No change	No change	++	+	−
South Europe-Mediterranean	++	++	++	+	−
North Asia (>45°N)	No change	No change/+	++	+	−
South Asia (<45°N)	+++	+++	+++	+++	−
Australia	++	++	+++	+++	−
Indonesia-Micronesia	++	++	+++	+++	++++
Pacific Ocean (30°S to 30°N)	++	++	+++	+++	−
Atlantic Ocean (30°S to 30°N)	+++	+++	++++	+++	−
Indian Ocean (30°S to 30°N)	++	+++	+++	+++	−
North Pole (>70°N)	+	+	++	No change	No change/−
South Pole (>70°S)	++	++	+++	No change	No change/−

Note. A + or a − sign stands for an increase or a decrease, respectively. The qualitative degree of increase/decrease is noted using: very weak: +/−, weak: ++/−−, small: +++/−−−, strong: ++++/−−−−. A "No change" is written when no variations in the densities studied are predicted. Note that the corresponding quantitative enhancements/decreases of the chemical species can be seen in previous figures. The symbols used here for the qualitative description were generated assuming the criterion that "very weak," "weak," "small," and "strong" roughly correspond to, respectively, <20%, 20–30%, 30–60%, and 75–100% of the absolute enhancement due to lightning in the species column density.

Inside the continents, where the amount of DMS is negligible, the lightning generated OH would destroy SO_2 through $SO_2 + OH \rightarrow SO_4$.

Tables 3 and 4 include a qualitative description of the chemical species analyzed in this work with an indication of the geographical regions where our CAM5 simulations predict general increases/decreases. The symbols used in Tables 3 and 4 for the qualitative description were generated assuming the criterion that "very weak," "weak," "small" and "strong" roughly correspond to, respectively, <20%, 20–30%, 30–60%, and 75–100% of the absolute enhancement due to lightning in the column density of the 9 species listed in Tables 3 and 4. The criterion is the same for all of the species.

In summary, we have explored the behavior of six different lightning parameterizations with CAM5. For this particular model, the global and land/ocean spatial correlations (with respect to OTD/LIS observations) of the different lightning schemes have been calculated. Our calculations may help to constrain the amount of LNO_x and how the lightning NO injected in the atmosphere influences the global concentrations of key chemical species such as OH, HO_2, H_2O_2, NO_x, O_3, SO_2, and HNO_3. Five out of the six lightning schemes investigated exhibit larger LNO_x in the midlatitudes than in the tropics. In particular, it is found that the ICEFLUX midlatitude LNO_x is 42% larger than its predicted tropical LNO_x. This is related to the predicted larger relative amount of cloud-to-ground (CG) lightning in midlatitude regions.

Our results suggest that, when using CAM5, the ICEFLUX lightning parameterization produces a total of 6.8 Tg N $year^{-1}$ and 337 mol NO $flash^{-1}$. Based on the ICEFLUX global and midlatitude spatial correlations of, respectively, 0.732 (the largest one) and 0.632 (well above 0.553 of CTH), it could be considered that ICEFLUX is the most reliable (with respect to OTD/LIS geographical distribution) lightning scheme among the tested ones in this study. Finally, the ICEFLUX scheme predicts an enhancement of ~38% (at ~7.5 km) in the concentration of tropospheric ozone (O_3) with respect to ambient values with no lightning and provides close agreement with ozone sonde measurements at 500 and 250 hPa (Finney et al., 2016).

Table 4
Indication—Based on the Six Lightning Schemes Investigated With CAM5—of the Geographical Regions of the World Where an Increase/Decrease of the Concentrations of H_2O_2, HNO_3, CO, and SO_2 Is Expected Due to Lightning

Geographical region	H_2O_2	HNO_3	CO	SO_2
North Africa	−	+ + +	− − −	No change
Central Africa	+	+ + +	− − −−	No change
South Africa	−	+ + +	− − −	No change
North-Eastern America	−	++	No change	No change
Gulf of Mexico	−	++	−−	No change
Central America (10°N - 20°N)	−	++	−−	No Change
South America (>30°S - 10°N)	+/++	++	− − −	+ (North Russia)
North Europe (>45°N)	−	++	No change	No change
South Europe - Mediterranean	+/−	+ + +	No change	++ (South Italy)
North Asia (> 45°N)	−	++	No change	− (Eastern China)
South Asia (< 45°N)	−	+ + +	− − −	No change
Australia	−/+	++	− − −	No change
Indonesia - Micronesia	+ + +	++	−−	No change
Pacific Ocean (30°S to 30°N)	−	++	− − −	No Change
Atlantic Ocean (30°S to 30°N)	−	+ + +	− − −	No Change
Indian Ocean (30°S to 30°N)	−	++	− − −	No Change
North Pole (>70°N)	No change	++	No change	No change
South Pole (>70°S)	No change	++	No change	No change

Note. A + or a − sign stands for an increase or a decrease, respectively. The qualitative degree of increase/decrease is noted using: very weak: +/−, weak: ++/−−, small: + + +/− − −, strong: + + + +/− − − −. A "No change" is written when no variations in the densities studied are predicted. Note that the corresponding quantitative enhancements/decreases of the chemical species can be seen in previous figures. The symbols used here for the qualitative description were generated assuming the criterion that "very weak," "weak," "small," and "strong" roughly correspond to, respectively, <20%, 20–30%, 30–60%, and 75–100% of the absolute enhancement due to lightning in the species column density.

To conclude, our ICEFLUX and CTH results agree with the enhancements of NO_2 and O_3 produced by lightning over tropical Atlantic and Africa and the weaker lightning background over the tropical Pacific reported by Martin et al. (2007). Martin et al. (2007) also indicated that a global source of 6 ± 2 Tg N year^{-1} from lightning best represented the satellite observations of tropospheric NO_2, O_3, and HNO_3 in the periods and locations where lightning is expected to dominate the trace gas observations.

References

Allen, D. J., & Pickering, K. E. (2002). Evaluation of lightning flash rate parameterizations for use in a global chemical transport model. *Journal of Geophysical Research: Atmospheres*, *107*(D23), 4711. https://doi.org/10.1029/2002JD002066

Allen, D. J., Pickering, K. E., Pinder, R. W., Henderson, B. H., Appel, K. W., & Prados, A. (2012). Impact of lightning-NO on eastern United States photochemistry during the summer of 2006 as determined using the CMAQ model. *Atmospheric Chemistry & Physics*, *12*, 1737. https://doi.org/10.5194/acp-12-1737-2012

Apel, E., Hornbrook, R., Hills, A., Blake, N., Barth, M., Weinheimer, A., et al. (2015). Upper tropospheric ozone production from lightning NO_x-impacted convection: Smoke ingestion case study from the DC3 campaign. *Journal of Geophysical Research: Atmospheres*, *120*, 2505–2523. https://doi.org/10.1002/2014JD022121

Arnone, E., Smith, A., Enell, C. F., Kero, A., & Dinelli, B. (2014). WACCM climate chemistry sensitivity to sprite perturbations. *Journal of Geophysical Research: Atmospheres*, *119*, 6958–6970. https://doi.org/10.1002/2013JD020825

Baehr, J., Schlager, H., Ziereis, H., Stock, P., van Velthoven, P., Busen, R., et al. (2003). Aircraft observations of NO, NO_y, CO, and O_3 in the upper troposphere from 60 ° N to 60 ° S-Interhemispheric differences at mitlatitudes. *Geophysical Research Letters*, *30*(11), 1598. https://doi.org/10.1029/2003GL016935

Barth, M. C., Cantrell, C. A., Brune, W. H., Rutledge, S. A., Crawford, J. H., Huntrieser, H., et al. (2015). The deep convective clouds and chemistry (DC3) field campaign. *Bulletin of the American Meteorological Society*, *96*(8), 1281–1309.

Beirle, S., Huntrieser, H., & Wagner, T. (2010). Direct satellite observation of lightning-produced NO_x. *Atmospheric Chemistry and Physics*, *10*(22), 10,965–10,986. https://doi.org/10.5194/acp-10-10965-2010

Beirle, S., Spichtinger, N., Stohl, A., Cummins, K., Turner, T., Boccippio, D., et al. (2006). Estimating the NO x produced by lightning from GOME and NLDN data: A case study in the Gulf of Mexico. *Atmospheric Chemistry and Physics*, *6*(4), 1075–1089.

Bovensmann, H., Burrows, J., Buchwitz, M., Frerick, J., Noël, S., Rozanov, V., et al. (1999). SCIAMACHY: Mission objectives and measurement modes. *Journal of the Atmospheric Sciences*, *56*(2), 127–150.

Acknowledgments
The authors acknowledge helpful discussions with Daniel Marsh, Michael Mills, Charles Bardeen, Douglas Kinnison, Rolando Garcia, Andrew Gettelman, Simone Tilmes, and Louisa Emmons. This work was supported by the Spanish Ministry of Science and Innovation, MINECO under Project ESP2017-86263-C4-4-R and by the EU through the H2020 Science and Innovation with Thunderstorms (SAINT) project (Ref. 722337) and the FEDER program. F. J. P. I. acknowledges support by a PhD research contract, Code BES-2014-069567 and by the EU through the European Research Council (ERC) under the European Union's H2020 programm/ERC Grant 681257. F. J. G. V. acknowledges support from the Spanish Ministry of Education and Culture under the Salvador de Madariaga Program PRX17/00078. Authors F. J. G. V. and F. J. P. I. acknowledge financial support from the State Agency for Research of the Spanish MCIU through the "Center of Excellence Severo Ochoa" award for the Instituto de Astrofísica de Andalucía (SEV-2017-0709). H. H. acknowledges support from the DLR project KliSAW. The National Center for Atmospheric Research is sponsored by the National Science Foundation. The CESM project is supported by the National Science Foundation and the Office of Science (BER) of the U.S. Department of Energy. Computing resources were provided by the Climate Simulation Laboratory at NCAR's Computational and Information Systems Laboratory (CISL), sponsored by the National Science Foundation and other agencies. Data presented here are available from figshare repository (https://bit.ly/2ww816g). Alternatively, requests for data and codes used to generate figures, graphs, plots, or tables may be made to the authors F. J. G. V (vazquez@iaa.es) or F. J. P. I. (fjpi@iaa.es).

Bucsela, E. J., Pickering, K. E., Huntemann, T. L., Cohen, R. C., Perring, A., Gleason, J. F., et al. (2010). Lightning-generated NOx seen by the Ozone Monitoring Instrument during NASA's Tropical Composition, Cloud and Climate Coupling Experiment (TC4). *Journal of Geophysical Research*, *115*, D00J10. https://doi.org/10.1029/2009JD013118

Burrows, J. P., Weber, M., Buchwitz, M., Rozanov, V., Ladstätter-Weißenmayer, A., Richter, A., et al. (1999). The global ozone monitoring experiment (GOME): Mission concept and first scientific results. *Journal of the Atmospheric Sciences*, *56*(2), 151–175.

Carey, L. D., Koshak, W., Peterson, H., & Mecikalski, R. M. (2016). The kinematic and microphysical control of lightning rate, extent, and NO_x production. *Journal of Geophysical Research: Atmospheres*, *121*, 7975–7989. https://doi.org/10.1002/2015JD024703

Cecil, D. J., Buechler, D. E., & Blakeslee, R. J. (2014). Gridded lightning climatology from TRMM-LIS and OTD: Dataset description. *Atmospheric Research*, *135*, 404. https://doi.org/10.1016/j.atmosres.2012.06.028

Chameides, W., Davis, D., Bradshaw, J., Rodgers, M., Sandholm, S., & Bai, D. (1987). An estimate of the NO_x production rate in electrified clouds based on NO observations from the GTE/CITE 1 fall 1983 field operation. *Journal of Geophysical Research*, *92*(D2), 2153–2156.

Christian, H. J., Blakeslee, R. J., Boccippio, D. J., Boeck, W. L., Buechler, D. E., Driscoll, K. T., et al. (2003). Global frequency and distribution of lightning as observed from space by the Optical Transient Detector. *Journal of Geophysical Research*, *108*(D1), 4005. https://doi.org/10.1029/2002JD002347

Clark, S. K., Ward, D. S., & Mahowald, N. M. (2017). Parameterization-based uncertainty in future lightning flash density. *Geophysical Research Letters*, *44*, 2893–2901. https://doi.org/10.1002/2017GL073017

Cooper, M., Martin, R. V., Wespes, C., Coheur, P. F., Clerbaux, C., & Murray, L. T. (2014). Tropospheric nitric acid columns from the IASI satellite instrument interpreted with a chemical transport model: Implications for parameterizations of nitric oxide production by lightning. *Journal of Geophysical Research: Atmospheres*, *119*, 10,068–10,079. https://doi.org/10.1002/2014JD021907

DeCaria, A. J., Pickering, K. E., Stenchikov, G. L., & Ott, L. E. (2005). Lightning-generated NO_x and its impact on tropospheric ozone production: A three-dimensional modeling study of a Stratosphere-Troposphere Experiment: Radiation, Aerosols and Ozone (STERAO-A) thunderstorm. *Journal of Geophysical Research*, *110*, D14303. https://doi.org/10.1029/2004JD005556

DeCaria, A. J., Pickering, K. E., Stenchikov, G. L., Scala, J. R., Stith, J. L., Dye, J. E., et al. (2000). A cloud-scale model study of lightning-generated NO_x in an individual thunderstorm during STERAO-A. *Journal of Geophysical Research*, *105*(D9), 11,601–11,616.

Defer, E., Blanchet, P., Théry, C., Laroche, P., Dye, J. E., Venticinque, M., & Cummins, K. L. (2001). Lightning activity for the July 10, 1996, storm during the Stratosphere-Troposphere Experiment: Radiation, Aerosol, and Ozone-A (STERAO-A) experiment. *Journal of Geophysical Research*, *106*(D10), 10,151–10,172.

Deierling, W., Petersen, W. A., Latham, J., Ellis, S., & Christian, H. J. (2008). The relationship between lightning activity and ice fluxes in thunderstorms. *Journal of Geophysical Research: Atmospheres*, *113*, D15210. https://doi.org/10.1029/2007JD009700

Emmons, L. K., Walters, S., Hess, P. G., Lamarque, J. F., Pfister, G. G., Fillmore, D., et al. (2010). Description and evaluation of the Model for Ozone and Related chemical Tracers, version 4 (MOZART-4). *Geoscientific Model Development*, *3*(1), 43–67. https://doi.org/10.5194/gmd-3-43-2010

Fehr, T., Höller, H., & Huntrieser, H. (2004). Model study on production and transport of lightning-produced NOx in a EULINOX supercell storm. *Journal of Geophysical Research*, *109*, D09102. https://doi.org/10.1029/2003JD003935

Finney, D., Doherty, R., Wild, O., & Abraham, N. L. (2016). The impact of lightning on tropospheric ozone chemistry using a new global lightning parametrisation. *Atmospheric Chemistry and Physics*, *16*(12), 7507–7522.

Finney, D. L., Doherty, R. M., Wild, O., Huntrieser, H., Pumphrey, H. C., & Blyth, A. M. (2014). Using cloud ice flux to parametrise large-scale lightning. *Atmospheric Chemistry and Physics. Discussions*, *14*, 17817. https://doi.org/10.5194/acpd-14-17817-2014

Finney, D. L., Doherty, R. M., Wild, O., Stevenson, D. S., MacKenzie, I. A., & Blyth, A. M. (2018). A projected decrease in lightning under climate change. *Nature Climate Change*, *8*(3), 210.

Franz, R. C., Nemzek, R. J., & Winckler, J. R. (1990). Television Image of a Large Upward Electrical Discharge Above a Thunderstorm System. *Science*, *249*, 48. https://doi.org/10.1126/science.249.4964.48

Goldenbaum, G., & Dickerson, R. (1993). Nitric oxide production by lightning discharges. *Journal of Geophysical Research*, *98*(D10), 18,333–18,338.

Gordillo-Vázquez, F. J., & Donkó, Z. (2009). Electron energy distribution functions and transport coefficients relevant for air plasmas in the troposphere: Impact of humidity and gas temperature. *Plasma Sources Science and Technology*, *18*(3), 034021. https://doi.org/10.1088/0963-0252/18/3/034021

Grewe, V. (2007). Impact of climate variability on tropospheric ozone. *Science of the Total Environment*, *374*(1), 167–181.

Grewe, V., Brunner, D., Dameris, M., Grenfell, J., Hein, R., Shindell, D., & Staehelin, J. (2001). Origin and variability of upper tropospheric nitrogen oxides and ozone at northern mid-latitudes. *Atmospheric Environment*, *35*(20), 3421–3433.

Grewe, V., Shindell, D., & Eyring, V. (2004). The impact of horizontal transport on the chemical composition in the tropopause region: lightning NOx and streamers. *Advances in Space Research*, *33*(7), 1058–1061.

Holmes, C., Brook, M., Krehbiel, P., & McCrory, R. (1971). On the power spectrum and mechanism of thunder. *Journal of Geophysical Research*, *76*(9), 2106–2115.

Huntrieser, H., Lichtenstern, M., Scheibe, M., Aufmhoff, H., Schlager, H., Pucik, T., et al. (2016b). On the origin of pronounced O_3 gradients in the thunderstorm outflow region during DC3. *Journal of Geophysical Research: Atmospheres*, *121*, 6600–6637. https://doi.org/10.1002/2015JD024279

Huntrieser, H., Lichtenstern, M., Scheibe, M., Aufmhoff, H., Schlager, H., Pucik, T., et al. (2016a). Injection of lightning-produced NO_x, water vapor, wildfire emissions, and stratospheric air to the UT/LS as observed from DC3 measurements. *Journal of Geophysical Research: Atmospheres*, *121*, 6638–6668. https://doi.org/10.1002/2015JD024273

Huntrieser, H., Schlager, H., Feigl, C., & Höller, H. (1998). Transport and production of NO_x in electrified thunderstorms: Survey of previous studies and new observations at midlatitudes. *Journal of Geophysical Research*, *103*(D21), 28,247–28,264.

Huntrieser, H., Schlager, H., Roiger, A., Lichtenstern, M., Schumann, U., Kurz, C., et al. (2007). Lightning-produced NO_x over Brazil during TROCCINOX: Airborne measurements in tropical and subtropical thunderstorms and the importance of mesoscale convective systems. *Atmospheric Chemistry and Physics*, *7*(1), 2561–2621.

Huntrieser, H., Schumann, U., Schlager, H., Höller, H., Giez, A., Betz, H. D., et al. (2008). Lightning activity in Brazilian thunderstorms during TROCCINOX: implications for NO_x production. *Atmospheric Chemistry and Physics*, *8*(4), 921–953. https://doi.org/10.5194/acp-8-921-2008

Inan, U. S., Barrington-Leigh, C., Hansen, S., Glukhov, V. S., Bell, T. F., & Rairden, R. (1997). Rapid lateral expansion of optical luminosity in lightning-induced ionospheric flashes referred to as 'elves'. *Geophysical Research Letters*, *24*, 583. https://doi.org/10.1029/97GL00404

Jorgensen, D. P., & LeMone, M. A. (1989). Vertical velocity characteristics of oceanic convection. *Journal of the Atmospheric Sciences*, *46*(5), 621–640.

Kar, S., Liou, Y. A., & Ha, K. J. (2007). Characteristics of cloud-to-ground lightning activity over Seoul, South Korea in relation to an urban effect. *Annales Geophysicae*, *25*, 2113–2118.

Khokhar, M., Frankenberg, C., Van Roozendael, M., Beirle, S., Kühl, S., Richter, A., et al. (2005). Satellite observations of atmospheric SO_2 from volcanic eruptions during the time-period of 1996–2002. *Advances in Space Research*, *36*(5), 879–887.

Kinnison, D., Brasseur, G., Walters, S., Garcia, R., Marsh, D., Sassi, F., et al. (2007). Sensitivity of chemical tracers to meteorological parameters in the MOZART-3 chemical transport model. *Journal of Geophysical Research*, *112*, D20302. https://doi.org/10.1029/2006JD007879

Koshak, W. (2014). *Global lightning nitrogen oxides production, chapter 19 of the lightning flash* (2nd ed., pp. 819). In V. Cooray (Ed.). Croydon, UK: The Institute of Engineering and Technology.

Koshak, W., Peterson, H., Biazar, A., Khan, M., & Wang, L. (2014). The NASA Lightning Nitrogen Oxides Model (LNOM): application to air quality modeling. *Atmospheric Research*, *135*, 363–369.

Kowalczyk, M., & Bauer, E. (1981). Lightning as a source of no sub x in the troposphere: INSTITUTE FOR DEFENSE ANALYSES ALEXANDRIA VA.

Labrador, L. J., von Kuhlmann, R., & Lawrence, M. G. (2004). Strong sensitivity of the global mean OH concentration and the tropospheric oxidizing efficiency to the source of NO_x from lightning. *Geophysical Research Letters*, *31*, L06102. https://doi.org/10.1029/2003GL019229

Labrador, L. J., von Kuhlmann, R., & Lawrence, M. G. (2005). The effects of lightning-produced NO_x and its vertical distribution on atmospheric chemistry: Sensitivity simulations with MATCH-MPIC. *Atmospheric Chemistry and Physics*, *5*(7), 1815–1834.

Lamarque, J. F., Emmons, L., Hess, P., Kinnison, D. E., Tilmes, S., Vitt, F., et al. (2012). CAM-chem: Description and evaluation of interactive atmospheric chemistry in the Community Earth System Model. *Geoscientific Model Development*, *5*(2), 369.

Levelt, P. F., van den Oord, G. H., Dobber, M. R., Malkki, A., Visser, H., de Vries, J., et al. (2006). The ozone monitoring instrument. *IEEE Transactions on Geoscience and Remote Sensing*, *44*(5), 1093–1101.

Liaskos, C. E., Allen, D. J., & Pickering, K. E. (2015). Sensitivity of tropical tropospheric composition to lightning NO_x production as determined by replay simulations with GEOS-5. *Journal of Geophysical Research: Atmospheres*, *120*, 8512–8534. https://doi.org/10.1002/2014JD022987

Liu, X., Easter, R. C., Ghan, S. J., Zaveri, R., Rasch, P., Shi, X., et al. (2012). Toward a minimal representation of aerosols in climate models: Description and evaluation in the Community Atmosphere Model CAM5. *Geoscientific Model Development*, *5*(3), 709.

Logan, J. A., Prather, M. J., Wofsy, S. C., & McElroy, M. B. (1981). Tropospheric chemistry: A global perspective. *Journal of Geophysical Research*, *86*(C8), 7210–7254.

Luke, W. T., Dickerson, R. R., Ryan, W. F., Pickering, K. E., & Nunnermacker, L. J. (1992). Tropospheric chemistry over the lower Great Plains of the United States 2. Trace gas profiles and distributions. *Journal of Geophysical Research*, *97*(D18), 20,647–20,670.

Marais, E. A., Jacob, D. J., Choi, S., Joiner, J., Belmonte-Rivas, M., Cohen, R. C., et al. (2018). Nitrogen oxides in the global upper troposphere: interpreting cloud-sliced NO_2 observations from the OMI satellite instrument. *Atmospheric Chemistry and Physics*, *18*(23), 1017–1027. https://doi.org/10.5194/acp-18-17017-2018

Marsh, D. R., Mills, M. J., Kinnison, D. E., Lamarque, J. F., Calvo, N., & Polvani, L. M. (2013). Climate change from 1850 to 2005 simulated in CESM1 (WACCM). *Journal of Climate*, *26*(19), 7372–7391.

Martin, R. V., Sauvage, B., Folkins, I., Sioris, C. E., Boone, C., Bernath, P., & Ziemke, J. (2007). Space-based constraints on the production of nitric oxide by lightning. *Journal of Geophysical Research*, *112*, D09309. https://doi.org/10.1029/2006JD007831

Martini, M., Allen, D. J., Pickering, K. E., Stenchikov, G. L., Richter, A., Hyer, E. J., & Loughner, C. P. (2011). The impact of North American anthropogenic emissions and lightning on long-range transport of trace gases and their export from the continent during summers 2002 and 2004. *Journal of Geophysical Research*, *116*, D07305. https://doi.org/10.1029/2010JD014305

Michalon, N., Nassif, A., Saouri, T., Royer, J., & Pontikis, C. (1999). Contribution to the climatological study of lightning. *Geophysical Research Letters*, *26*(20), 3097–3100.

Miyazaki, K., Eskes, H., Sudo, K., Boersma, K. F., Bowman, K., & Kanaya, Y. (2017). Decadal changes in global surface NO_x emissions from multi-constituent satellite data assimilation. *Atmospheric Chemistry and Physics*, *17*(2), 807–837.

Murray, L. T. (2016). Lightning NOx and impacts on air quality. *Current Pollution Reports*, *2*(2), 115–133.

Nault, B., Laughner, J., Wooldridge, P., Crounse, J., Dibb, J., Diskin, G., et al. (2017). Lightning NO_x Emissions: Reconciling measured and modeled estimates with updated NO_x chemistry. *Geophysical Research Letters*, *44*, 9479–9488. https://doi.org/10.1002/2017GL074436

Nesbitt, S., Salio, P., Varble, A., Trapp, R., Roberts, R., Dominguez, F., et al. (2017). Improving high impact weather and climate prediction for societal resilience in Subtropical South America: Project RELAMPAGO-CACTI. In *Agu fall meeting abstracts*.

Orville, R. E., Huffines, G., Nielsen-Gammon, J., Zhang, R., Ely, B., Steiger, S., et al. (2001). Enhancement of cloud-to-ground lightning over Houston, Texas. *Geophysical Research Letters*, *28*(13), 2597–2600.

Ott, L. E., Pickering, K. E., Stenchikov, G. L., Allen, D. J., DeCaria, A. J., Ridley, B., et al. (2010). Production of lightning NO_x and its vertical distribution calculated from three-dimensional cloud-scale chemical transport model simulations. *Journal of Geophysical Research*, *115*, D04301. https://doi.org/10.1029/2009JD011880

Ott, L. E., Pickering, K. E., Stenchikov, G. L., Huntrieser, H., & Schumann, U. (2007). Effects of lightning NO_x production during the 21 July European Lightning Nitrogen Oxides Project storm studied with a three-dimensional cloud-scale chemical transport model. *Journal of Geophysical Research*, *112*, D05307. https://doi.org/10.1029/2006JD007365

Ott, L., Pickering, K., Stenchikov, G., Lin, R., Ridley, B., Loewenstein, M., et al. (2005). The impact of lightning NO x production on atmospheric chemistry in a CRYSTAL-FACE thunderstorm simulated using a 3-D cloud-scale chemical transport model. In *AMS Conference on Meteor. Appl. Of Lightning Data*, San Diego, California. http://ams.confex.com/ams/Annual2005/techprogram/paper_84679.htm

Parra-Rojas, F. C., Luque, A., & Gordillo-Vázquez, F. J. (2013). Chemical and electrical impact of lightning on the Earth mesosphere: The case of sprite halos. *Journal of Geophysical Research: Space Phys*, *118*, 5190–5214. https://doi.org/10.1002/jgra.50449

Pérez-Invernón, F. J., Gordillo-Vázquez, F. J., Smith, A. K., Arnone, E., & Winkler, H. (2019). Global occurrence and chemical impact of stratospheric Blue Jets modeled with WACCM4. *Journal of Geophysical Research: Atmospheres*, *124*, 2841–2864. https://doi.org/10.1029/2018JD029593

Pérez-Invernón, F. J., Luque, A., & Gordillo-Vázquez, F. J. (2018). Modeling the chemical impact and the optical emissions produced by lightning-induced electromagnetic fields in the upper atmosphere: The case of halos and elves triggered by different lightning discharges. *Journal of Geophysical Research: Atmospheres*, *123*, 7615–7641. https://doi.org/10.1029/2017JD028235

Pickering, K. E., Bucsela, E. J., Allen, D. J., Holzworth, R. H., & Krotkov, N. A. (2018). Lightning NO_x Production per Flash in the Midlatitudes and Tropics Derived from OMI NO_2, and WWLLN Observations. https://ams.confex.com/ams/98Annual/webprogram/Paper331166.html

Pickering, K. E., Bucsela, E., Allen, D., Ring, A., Holzworth, R., & Krotkov, N. (2016). Estimates of lightning NO_x production based on OMI NO_2 observations over the Gulf of Mexico. *Journal of Geophysical Research: Atmospheres*, *121*, 8668–8691. https://doi.org/10.1002/2015JD024179

Pickering, K. E., Thompson, A. M., Wang, Y., Tao, W. K., McNamara, D. P., Kirchhoff, V. W., et al. (1996). Convective transport of biomass burning emissions over Brazil during TRACE A. *Journal of Geophysical Research*, *101*(D19), 23,993–24,012.

Pickering, K. E., Wang, Y., Tao, W. K., Price, C., & Müller, J. F. (1998). Vertical distributions of lightning NO_x for use in regional and global chemical transport models. *Journal of Geophysical Research*, *103*(D23), 31,203–31,216.

Pollack, I., Homeyer, C., Ryerson, T., Aikin, K., Peischl, J., Apel, E., et al. (2016). Airborne quantification of upper tropospheric NO_x production from lightning in deep convective storms over the United States Great Plains. *Journal of Geophysical Research: Atmospheres*, *121*, 2002–2028. https://doi.org/10.1002/2015JD023941

Price, C., Penner, J., & Prather, M. (1997). NO_x from lightning: 1. Global distribution based on lightning physics. *Journal of Geophysical Research*, *102*(D5), 5929–5941.

Price, C., & Rind, D. (1992). A simple lightning parameterization for calculating global lightning distributions. *Journal of Geophysical Research*, *97*(D9), 9919–9933.

Price, C., & Rind, D. (1993). What determines the cloud-to-ground lightning fraction in thunderstorms?. *Geophysical Research Letters*, *20*(6), 463–466.

Rakov, V. A., & Uman, M. A. (Eds.) (2003). *Lightning Physics and Effects*. Cambridge: Cambridge University Press.

Redelsperger, J. L., Thorncroft, C. D., Diedhiou, A., Lebel, T., Parker, D. J., & Polcher, J. (2006). African Monsoon Multidisciplinary Analysis: An international research project and field campaign. *Bulletin of the American Meteorological Society*, *87*(12), 1739–1746.

Richter, A., Burrows, J. P., Nüß, H., Granier, C., & Niemeier, U. (2005). Increase in tropospheric nitrogen dioxide over China observed from space. *Nature*, *437*(7055), 129.

Richter, J. H., & Rasch, P. J. (2008). Effects of convective momentum transport on the atmospheric circulation in the Community Atmosphere Model, version 3. *Journal of Climate*, *21*(7), 1487–1499.

Ridley, B., Pickering, K., & Dye, J. (2005). Comments on the parameterization of lightning-produced NO in global chemistry-transport models. *Atmospheric Environment*, *39*(33), 6184–6187.

Romps, D. M., Charn, A. B., Holzworth, R. H., Lawrence, W. E., Molinari, J., & vollaro, D. (2018). CAPE times P explains lightning over land but not the land-ocean contrast. *Geophysical Research Letters*, *45*, 12,623–12,630. https://doi.org/10.1029/2018GL080267

Romps, D. M., Seeley, J. T., Vollaro, D., & Molinari, J. (2014). Projected increase in lightning strikes in the United States due to global warming. *Science*, *346*(6211), 851–854. https://doi.org/10.1126/science.1259100

Rossow, W. B., & Schiffer, R. A. (1991). ISCCP cloud data products. *Bulletin of the American Meteorological Society*, *72*(1), 2–20.

Sander, S., Abbatt, J., Barker, J., Burkholder, J., Friedl, R., Golden, D., et al. (2011). Chemical kinetics and photochemical data for use in Atmospheric Studies Evaluation Number 17, JPL Publication 10-6, Jet Propulsion Laboratory, Pasadena. Pasadena, CA: Jet Propulsion Laboratory, National Aeronautics and Space Administration. http://jpldataeval.jpl.nasa.gov

Schumann, U., & Huntrieser, H. (2007). The global lightning-induced nitrogen oxides source. *Atmospheric Chemistry and Physics*, *7*(14), 3823–3907. https://doi.org/10.5194/acp-7-3823-2007

Seltzer, K., Vizuete, W., & Henderson, B. (2015). Evaluation of updated nitric acid chemistry on ozone precursors and radiative effects. *Atmospheric Chemistry and Physics*, *15*(10), 5973–5986.

Soriano, L. R., & de Pablo, F. (2002). Effect of small urban areas in central Spain on the enhancement of cloud-to-ground lightning activity. *Atmospheric Environment*, *36*(17), 2809–2816.

Steiger, S. M., Orville, R. E., & Huffines, G. (2002). Cloud-to-ground lightning characteristics over Houston, Texas: 1989–2000. *Journal of Geophysical Research*, *107*(D11), ACL 2–1–ACL 2–12. https://doi.org/10.1029/2001JD001142

Tilmes, S., Lamarque, J. F., Emmons, L., Kinnison, D., Ma, P., Liu, X., et al. (2015). Description and evaluation of tropospheric chemistry and aerosols in the Community Earth System Model (CESM1. 2). *Geoscientific Model Development*, *8*(5), 1395.

Tilmes, S., Lamarque, J. F., Emmons, L. K., Kinnison, D. E., Marsh, D., Garcia, R. R., et al. (2016). Representation of the Community Earth System Model (CESM1) CAM4-chem within the Chemistry-Climate Model Initiative (CCMI). *Geoscientific Model Development*, *9*(5), 1853–1890.

Torres, A., & Buchan, H. (1988). Tropospheric nitric oxide measurements over the Amazon Basin. *Journal of Geophysical Research*, *93*(D2), 1396–1406.

Tost, H., Jöckel, P., & Lelieveld, J. (2007). Lightning and convection parameterisations–uncertainties in global modelling. *Atmospheric Chemistry and Physics*, *7*(17), 4553–4568.

Vonnegut, B. (1963). Some facts and speculations concerning the origin and role of thunderstorm electricity, *Severe Local Storms* (pp. 224–241). Boston, MA: Springer.

Voulgarakis, A., Naik, V., Lamarque, J. F., Shindell, D. T., Young, P., Prather, M. J., et al. (2013). Analysis of present day and future OH and methane lifetime in the ACCMIP simulations. *Atmospheric Chemistry and Physics*, *13*(5), 2563–2587.

Wang, Y., DeSilva, A., Goldenbaum, G., & Dickerson, R. (1998). Nitric oxide production by simulated lightning: Dependence on current, energy, and pressure. *Journal of Geophysical Research*, *103*(D15), 19,149–19,159.

Wescott, E. M., Sentman, D., Osborne, D., Hampton, D., & Heavner, M. (1995). Preliminary results from the Sprites94 aircraft campaign: 2. Blue jets. *Geophysical Research Letters*, *22*, 1209. https://doi.org/10.1029/95GL00582

Westcott, N. E. (1995). Summertime cloud-to-ground lightning activity around major Midwestern urban areas. *Journal of Applied Meteorology and Climatology*, *34*(7), 1633–1642.

Wild, O. (2007). Modelling the global tropospheric ozone budget: exploring the variability in current models. *Atmospheric Chemistry and Physics*, *7*(10), 2643–2660.

Williams, E. R. (1985). Large-scale charge separation in thunderclouds. *Journal of Geophysical Research*, *90*(D4), 6013–6025.

Yoshida, S., Morimoto, T., Ushio, T., & Kawasaki, Z. (2009). A fifth-power relationship for lightning activity from Tropical Rainfall Measuring Mission satellite observations. *Journal of Geophysical Research*, *114*, D09104. https://doi.org/10.1029/2008JD010370

Zhang, G. J., & McFarlane, N. A. (1995). Sensitivity of climate simulations to the parameterization of cumulus convection in the Canadian Climate Centre general circulation model. *Atmos. Ocean*, *33*(3), 407–446.